For Reference

NOT TO BE TAKEN FROM THIS ROOM

For Reference

NOT TO BE TAKEN FROM THIS ROOM

Ex libris
universitatis
albertaensis

UNIVERSITY OF ALBERTA
QUAECUMQUE VERA

University of Alberta
Printing Department

Thesis
1959(F)
#35

THE UNIVERSITY OF ALBERTA

"THE EFFECT OF ROCK PROPERTIES ON BACTERIA PLUGGING IN RESERVOIR ROCKS"

BY

JAMES T. RALEIGH

A THESIS
SUBMITTED TO THE FACULTY OF GRADUATE STUDIES
IN PARTIAL FULFILLMENT OF
THE REQUIREMENTS FOR THE DEGREE OF
MASTER OF SCIENCE IN PETROLEUM ENGINEERING

FACULTY OF ENGINEERING
DEPARTMENT OF CHEMICAL AND PETROLEUM ENGINEERING

EDMONTON, ALBERTA
AUGUST, 1959

Digitized by the Internet Archive
in 2018 with funding from
University of Alberta Libraries

https://archive.org/details/effectofrockprop00jame

Thesis
1962(F)
#59.

THE UNIVERSITY OF ALBERTA

"THE EFFECT OF ROCK PROPERTIES ON BACTERIA PLUGGING IN RESERVOIR ROCKS"

BY

JAMES T. RALEIGH

A THESIS
SUBMITTED TO THE FACULTY OF GRADUATE STUDIES
IN PARTIAL FULFILLMENT OF
THE REQUIREMENTS FOR THE DEGREE OF
MASTER OF SCIENCE IN PETROLEUM ENGINEERING

FACULTY OF ENGINEERING
DEPARTMENT OF CHEMICAL AND PETROLEUM ENGINEERING

EDMONTON, ALBERTA
AUGUST, 1962

ABSTRACT

The plugging process in reservoir rocks immediately adjacent to water injection well bores is not completely understood. This study investigated the nature of injection plugging and attempted to relate its characteristics to physical rock properties. Four specific formation types were defined and plugged; two were fairly uniform-grained sandstones and two were heterogeneous carbonates. The solids used for plugging were a commonly-occurring, uniform-sized dead bacteria, Bacillus subtilis. Injection rate and concentration of solids in brine were held constant during test runs.

Experimental results based on desaturation capillary pressure curves indicated that the two types of carbonate rocks used in this study had multi-pore systems. Wettability imbibition tests indicated that the Devonian and Cardium cores were less water-wet than the Indiana and Berea cores. This wettability difference affected the shape and location of the capillary pressure curves and dependent properties.

Plugging test results indicated that depth of plugging was a function of the pore geometry factor "G". Rate of plugging was dependent not only on the pore geometry, but also on the distribution and rate of change of the large pore channels to small pores. No correlation was found between rate of plugging and permeability, irreducible water saturation, or "G" factor. The "G" factor does not appear to completely define porous rock geometry for plugging predictions.

ACKNOWLEDGEMENTS

The writer wishes to express sincere appreciation to the following:

Dr. D. L. Flock for his guidance and constructive advice throughout this project.

Dr. G. E. Myers and the staff of the Department of Bacteriology for supplying the micro-organisms and for counsel on bacteria.

Dr. Walter Nader for his suggestions and interest.

Messrs. F. Butz, C. R. Kirby and all the members of the Department Technical Staff for their assistance and advice in the design and construction of equipment.

Mr. B. P. Shields for reviewing the manuscript.

The many friends and colleagues who provided valuable advice and criticism.

Doris Mary, my wife, for her typing, drafting and especially for her encouragement.

The financial assistance of the University of Alberta and the National Research Council is gratefully acknowledged.

TABLE OF CONTENTS

Page

ABSTRACT a

ACKNOWLEDGEMENTS b

LIST OF TABLES i

LIST OF FIGURES iii

INTRODUCTION 1

RESERVOIR ROCK PROPERTIES
- General 4
- Porosity 5
- Permeability 6
- Wettability 7
- Capillary Pressure 8
- Pore Geometry Factor 11

PROPERTIES OF BRINE AND BACTERIA
- Brine 16
- Bacteria 17

EXPERIMENTAL APPARATUS AND PROCEDURES
- Rock Property Determinations 20
- Permeability, Plugging and Backwashing 23

DISCUSSION OF RESULTS
- Capillary Pressure Curves 29
- Effects of Wettability 38
- Plugging Results 43
- Backwashing Results 61

CONCLUSIONS 64

RECOMMENDATIONS 68

NOMENCLATURE 70

BIBLIOGRAPHY 72

APPENDIX 75

LIST OF TABLES

Table	Title	Page
1	Summary of Rock Properties	56
2	Capillary Pressure Curve Data for Core No. 1 - 1	A 1
3	Capillary Pressure Curve Data for Core No. 1 - 3	A 2
4	Capillary Pressure Curve Data for Core No. 1 - 4	A 4
5	Capillary Pressure Curve Data for Core No. 1 - 6 using Mercury	A 5
6	Capillary Pressure Curve Data for Core No. 2 - 2	A 7
7	Capillary Pressure Curve Data for Core No. 2 - 4	A 9
8	Capillary Pressure Curve Data for Core No. 2 - 5	A 10
9	Capillary Pressure Curve Data for Core No. 2 - 7 using Mercury	A 11
10	Capillary Pressure Curve Data for Core No. 4 - 1	A 12
11	Capillary Pressure Curve Data for Core No. 4 - 2	A 14
12	Capillary Pressure Curve Data for Core No. 4 - 4	A 16
13	Capillary Pressure Curve Data for Core No. 4 - 5	A 17
14	Capillary Pressure Curve Data for Core No. 4 - 8 using Mercury	A 18
15	Capillary Pressure Curve Data for Core No. 5 - 2	A 20
16	Capillary Pressure Curve Data for Core No. 5 - 4 using Mercury	A 21
17	Capillary Pressure Curve Data for Core No. 7 - 3	A 23
18	Capillary Pressure Curve Data for Core No. 7 - 4	A 24
19	Imbibition Data for Core No. 1 - 4	A 26
20	Imbibition Data for Core No. 2 - 5	A 27

Table	Title	Page
21	Permeability and Plugging Data for Core No. 1 - 1	A 28
22	Permeability and Plugging Data for Core No. 1 - 3	A 29
23	Permeability and Plugging Data for Core No. 1 - 4	A 30
24	Permeability and Plugging Data for Core No. 2 - 2	A 31
25	Permeability and Plugging Data for Core No. 2 - 4	A 32
26	Permeability and Plugging Data for Core No. 2 - 5	A 33
27	Permeability and Plugging Data for Core No. 2 - 6	A 34
28	Permeability and Plugging Data for Core No. 4 - 1	A 35
29	Permeability and Plugging Data for Core No. 4 - 3	A 36
30	Permeability and Plugging Data for Core No. 4 - 5	A 37
31	Permeability and Plugging Data for Core No. 4 - 6	A 38
32	Permeability and Plugging Data for Core No. 5 - 2	A 39
33	Permeability and Plugging Data for Core No. 5 - 3	A 40
34	Permeability and Plugging Data for Core No. 7 - 3	A 41
35	Permeability and Plugging Data for Core No. 7 - 4	A 42
36	Backwashing Data on Core No. 1 - 3	A 43
37	Backwashing Data on Core No. 2 - 6	A 44
38	Backwashing Data on Core No. 4 - 3	A 45
39	Backwashing Data on Core No. 5 - 3	A 46

LIST OF FIGURES

Figure	Title	Page
1	Family of Computed Capillary Pressure Curves	15
2	Schematic Sketch of Plugging Apparatus	24
3	Capillary Pressure Curve for Core No. 1 - 1	30
4	Capillary Pressure Curve for Core No. 2 - 4	31
5	Capillary Pressure Curve for Core No. 4 - 4	32
6	Capillary Pressure Curve for Core No. 7 - 3	33
7	Capillary Pressure Curve for Core No. 2 - 5 and Comparison to Mercury Injection Curve for Core No. 2 - 7	35
8	Imbibition Curves for Water-Wet Cores	39
9	Plugging Pressure Profile for Core No. 5 - 3	45
10	Plugging Pressure Profile for Core No. 4 - 6	46
11	Plugging Pressure Profile for Core No. 1 - 3	47
12	Plugging Pressure Profile for Core No. 2 - 2	48
13	Plugging Plot for Devonian Cores	51
14	Plugging Plot for Indiana Cores	52
15	Plugging Plot for Berea Cores	53
16	Plugging Plot for Cardium Cores	54
17	Plugging Plot for All Cores with a Permeability Parameter	57
18	Plugging Plot for All Cores with an Irreducible Water Saturation Parameter	58

Figure	Title	Page
19	Plugging Plot for All Cores with a Pore Geometry Factor Parameter	59
20	Backwashing Plot for Various Cores	62
21	Capillary Pressure Curve for Core No. 1 - 3	A 3
22	Capillary Pressure Curve for Core No. 1 - 4 and Comparison to Mercury Injection Curve for Core No. 1 - 6	A 6
23	Capillary Pressure Curve for Core No. 2 - 2	A 8
24	Capillary Pressure Curve for Core No. 4 - 1	A 13
25	Capillary Pressure Curve for Core No. 4 - 2	A 15
26	Capillary Pressure Curve for Core No. 4 - 5 and Comparison to Mercury Injection Curve for Core No. 4 - 8	A 19
27	Capillary Pressure Curve for Core No. 5 - 2 and Comparison to Mercury Injection Curve for Core No. 5 - 4	A 22
28	Capillary Pressure Curve for Core No. 7 - 4	A 25

INTRODUCTION

Injection of water into oil bearing formations is common practice in the petroleum industry. There are a number of operational problems involved with water injection wells. One of the most serious is the tendency of the porous rock immediately adjacent to the injection well bore to partially plug off. This will result in increased injection pressures and/or a decrease in the rate of injection.

Plugging in injection wells can be the result of four major causes(5)*:

(1) Water can contain acid gases, carbon dioxide, hydrogen sulphide and/or oxygen. The problem is one of down-hole corrosion. The result of the steel corrosion causes clogging of injection wells with rust and scale.

(2) Water can contain barium, strontium, iron and calcium in solution along with the sulphate, sulfide, carbonate and oxide radicals. These ions, in combination with those present in the flood reservoir, can result in precipitation of compounds which plug the well bore face and may also plug out into the reservoir body itself.

(3) Water can contain suspended materials which could promptly and effectively plug the injection well.

(4) Water can contain algae, bacteria and other micro-organisms

*Numbers in brackets refer to references in Bibliography at end of text.

in sufficient quantities to plug the formation. Also, bacteria can live and grow in the reservoir environment to the extent of choking off the injection well. Some bacteria generate corrosive hydrogen sulphide.

Knowledge of the plugging process in porous rock is rather limited; most of the work to date is confined to formation damage due to drilling fluid and mud particle invasion(12). One of the main purposes of drilling mud is to line the drilled hole with an impermeable filter cake. It is in satisfying this function that formation plugging occurs. Plugging in injection wells is the result of a different objective. It occurs as a result of fluid injection radially into the formation.

The purpose of this work was to investigate the nature of injection plugging and to attempt to relate its characteristics to physical rock properties. A large number of variables exist in research of this type and in order to reduce them, injection rate and concentration of solids in brine were held constant. The solids used for plugging were a uniform sized dead bacteria, Bacillus subtilis, a micro-organism commonly found in water, air and soils. Four specific porous rock types were plugged; two were consolidated sandstones and two were heterogeneous carbonates.

The experimental work involved two distinct phases. The first concerned determining the physical rock properties: porosity,

capillary pressure, wettability and permeability of the cores. From the capillary pressure curves, a pore geometry factor and irreducible water saturation were obtained. The second phase of the experimental work was the actual plugging and backwashing of the selected core samples. This yielded information with respect to plugging penetration depth, and permeability reduction as a function of pore volumes injected.

RESERVOIR ROCK PROPERTIES

General

Uren(30) has defined a petroleum reservoir as: "..... a body of porous and permeable rock containing oil and gas through which fluids may move toward recovery openings under the pressure existing or that may be applied..... The reservoir rocks are usually semi-consolidated sands, sandstones, conglomerates, limestones or dolomites which offer sufficient pore space to permit the storage of fluids within them..... and having rock openings sufficiently large and continuous to allow movement of fluids through them." The basic properties are porosity and permeability. However, in this study some knowledge of wettability, capillary pressure curve characteristics and pore geometry are also required. These latter two are, in part, functions of permeability and porosity. Wettability is largely controlled by compounds adsorbed by the rock surfaces(4).

The voids within porous rock can be classified in three groups according to their size, based on the behavior of fluids within the void space(9). In the smallest void spaces molecular forces between the molecules of the rock solid and those of the fluid are very significant. These tiniest void spaces are termed molecular interstices or force spaces. In the largest void spaces the motion of the

fluid is insignificantly affected by the confining walls. These largest void spaces are referred to as caverns. Those spaces which are intermediate in size between molecular interstices and caverns are termed pores or capillaries. These capillaries are most important from a reservoir engineering viewpoint and the pore walls do have a significant affect on the hydrodynamic behavior in their interior.

Porosity

Total porosity(1) of a reservoir rock is defined as the ratio of the void space in a rock to the bulk volume expressed in per cent. Effective porosity is the ratio of the interconnected void space in the rock to the bulk volume of the rock expressed in per cent. For engineering work, effective porosity is the quantitative value desired as this represents the space which can be occupied by mobile fluids.

Porosity may be classified according to the mode of origin as original or induced. Original porosity is that developed in the deposition of the material, while induced porosity is that developed by some geologic process subsequent to deposition of the rock. Original porosity is typified by the intergranular porosity of sandstones and the intercrystalline and oolitic porosity of some limestones. Induced porosity is typified by fracture development as found in some shales and

by the vugs or solution cavities commonly found in limestones. Rocks having original porosity are more uniform in their characteristics than those in which a large part of the porosity is secondary or induced.

Pirson(23) has outlined eight distinguishable types of porosity in carbonate reservoirs. These have been sub-divided into three groups of primary porosities and five of secondary porosities. As porosity in carbonate reservoirs is mostly developed through circulating waters, these waters can also cause infilling of previously existing pores with chert, salt, anhydrite and gypsum.

Permeability

API Code 27(25) states that permeability is a property of the porous medium and is a measure of the capacity of the medium to transmit fluids. Permeability is the fluid conductivity of the reservoir rock. Permeability is defined mathematically from Darcy's Law:

$$K = \frac{Q\mu L}{A\,(\Delta P)}$$

Where: K = permeability in darcys.
Q = flow rate in cc/sec.
ΔP = pressure differential in atm.
L = core length in cms.
A = cross-sectional area of the core in square cms.
μ = viscosity in centipoises.

The darcy is a unit of dimension length squared. It is defined as the

permeability of a material that will produce a flow rate of one cubic centimetre of fluid per second with one centipoise viscosity through a cube having sides one centimetre in length, due to a pressure differential of one atmosphere. The permeability term in common use is the millidarcy which is equal to 0.001 darcy.

Generally, permeability must be determined by the geometry of the porous structure in a more or less statistical fashion. It should be proportional to some sort of mean square pore diameter or pore radius squared. The spread of pore sizes is also an important factor in the determination of permeability.

Wettability

Wettability(12) refers to the relative affinity between the rock and each fluid present, i.e., which fluid is preferentially adsorbed on the rock surface and is held in the most minute portions of the intersticies.

Wettability may be imagined in terms of a contact angle. If two fluid phases, water and oil, are at one point in contact with a solid, then, at equilibrium conditions, the two fluid phases will form a definite angle with the solid. This angle measured from the solid through the liquid phase of greatest density has been termed the contact

angle. Usually, the properties of the solid are such that it makes the contact angle less than 90 degrees toward one of the fluid phases. The solid has a preferential wettability to that phase. For example, if the contact angle relative to the water phase is less than 90 degrees, the rock is termed preferentially water-wet. The water will tend to displace oil from the rock surface because of its affinity for the rock. Wettability has a relative meaning only and is subject to hysteresis in much the same manner as surface tensions(27).

Within a porous solid which has different types of solid surfaces and many shapes of pores, the problem of relative wettability becomes quite complex. It is not practical to assume that the relative wettability could be stated in terms of a single contact angle even if such an angle could be measured. In spite of the complexity it has been possible by some performance and/or imbibition tests to determine the indicated preferential wettability(7).

Capillary Pressure

When two immiscible fluids are in contact in a porous media a difference in pressure exists between the two fluids which depends upon the curvature of the interface separating the fluids(9). This differential pressure is called capillary pressure.

A simpler expression for capillary pressure is that pressure which is necessary to displace a wetting fluid from a capillary opening. The significance of capillary pressure becomes apparent when one considers that most petroleum reservoirs may be visualized as a heterogeneous and tortuous bundle of capillary tubes. The factors which govern capillary pressure are the surface or interfacial tension of the fluids involved, the system wettability and the equivalent pore radius(12).

Thus: $$P_c = \frac{2\sigma \cos \theta}{r}$$

Where:
P_c = capillary pressure.
σ = interfacial tension between the two fluids involved.
θ = contact angle.
r = radius of the capillary.

When two immiscible fluids are in contact, there is free interfacial energy present between them. This interfacial energy arises from the net inward attraction of the interior molecules of a fluid upon those at its surface. This results in the tendency of a liquid to contract and expose a minimum free surface. It is a "skin effect" at the surface or interface, similar to the tension of a stretched membrane. The interfacial tension resulting from these free interfacial forces is a governing factor in the value of capillary pressure.

Often, when considering capillary pressure as applied to

porous media, the preceding equation is altered to the following form:

$$P_c = \sigma \left(\frac{1}{r_1} + \frac{1}{r_2} \right)$$

where r_1 and r_2 are the radii of curvature of the interface between the two fluids present. The term $\left[1/r_1 + 1/r_2\right]$ may be considered as the mean curvature of the surface. Any change in saturation within the system will change the interface radii and also the capillary pressure. Capillary pressure is, therefore, a function of saturation.

The displacement of one fluid by another in the pores of a porous medium is either aided or opposed by the surface forces of capillary pressure. As a consequence, in order to maintain a porous medium partially saturated with non-wetting fluid, while the medium is also exposed to wetting fluid, it is necessary to maintain the pressure of the non-wetting fluid at a value greater than that in the wetting fluid. The pressure in the wetting phase fluid is denoted by P_w and that in the non-wetting phase by P_{nw}, it follows that:

$$P_c (S_w) = P_{nw} - P_w$$

That is, the pressure differential between the two fluid phases is the capillary pressure which is a function of saturation. This is the defining equation for capillary pressure in a porous media.

Pore Geometry Factor

In general, not considering cavernous and highly fractured reservoirs, petroleum engineering deals with the capillary type pore spaces in porous media. Unfortunately, these pore systems of hydrocarbon reservoirs form an extremely complicated surface, geometrically difficult to describe. Indeed, it seems impossible to find any simple parameter or function to describe this highly irregular interconnected pore shape(27). However, the shape character of the capillary pressure curve can be interpreted in terms of pore geometry.

Capillary forces will oppose the entrance of a non-wetting phase fluid into a small pore filled with wetting phase fluid. However, this opposition may be overcome by the application of external pressure to the non-wetting phase. The pressure that is required to displace the wetting phase fluid from a pore, with non-wetting phase fluid, is an indication of the equivalent pore entry radius or cross-sectional area of the pore. This basic concept is utilized to show that the shape and location of the capillary pressure curve depends on the interconnection of the pores and the pore size distribution.

The sketch shown on the following page has two capillary pressure curves from two different reservoirs, "A" and "B", based on core specimens. The displacement pressure (D.P.) is the minimum

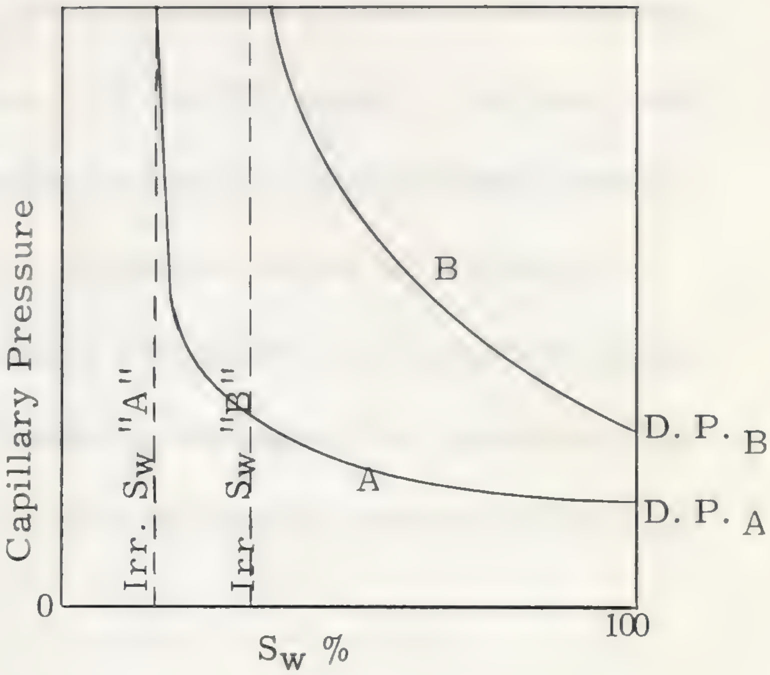

pressure at which the non-wetting phase fluid will enter the core saturated with the wetting phase. It is an indication of the largest cross-sectional area of pore entry at the sample surface. The slow rise in curve "A" indicates that a large percentage of the pore system has the same effective radius and geometry. This is indicative of a rather homogeneous porous media such as a clean, uniform grained, well sorted sandstone. The rather rapid rise in curve "B" suggests a continuous decrease in effective pore sizes entered by the non-wetting fluid. This is indicative of a heterogeneous porous media as a sandstone with a gradation in sizes of grains and pores and of variable permeability due to the presence of clay and matrix material. The irreducible wetting phase saturation of "A" is considerably lower than that of "B" because the effective interconnected pore volume is a higher percentage of effective porosity than that of "B". This can be expected because the pore geometry of "B" is more heterogeneous than that of "A".

Pore size distribution curves calculated from capillary

pressure information(6) suffer from a serious limitation which applies to all attempts to define pore size with finite figures. The pore entry is treated as cylindrical and certainly this is a gross simplification. The complexity of natural porous structures defies all attempts to define "pore size". Even so, simple definitions such as those which will be applied have some utility and contribute to the understanding of the part played by pore size in determining the characteristics of plugging in porous rocks.

Thomeer(28) utilized the idea that the location and shape of the capillary pressure curve reflects characteristics of the pore structure of any porous media sample. A mathematical description of capillary pressure curves and of indicated differences in pore geometry of samples was presented. He plots capillary pressure versus fractional bulk volume occupied by the displacing fluid. By using the fractional bulk concept, porosity of the sample is incorporated into the plot. When the measured values of P_c and $(V_b)_{P_c}$ of numerous core samples were plotted on log-log paper, the best fitting curve approximated a hyperbola. The modified mathematical expression to describe these curves was:

$$\frac{(V_b)_{P_c}}{(V_b)_{P_\infty}} = e^{-G/(\log P_c/P_d)}$$

Where $(V_b)_{P_c}$ = fractional bulk volume occupied by the displacing fluid at P_c.

$(V_b)_{P_\infty}$ = fractional bulk volume occupied at infinite pressure or total interconnected pore volume.

P_c = capillary pressure at any fractional volume displaced.

P_d = displacement pressure.

G = pore geometry factor.

The shape of the curve is defined by the pore geometry factor "G". The curve shape as discussed is related directly to the sorting and interconnection of the pores of the sample. The location of an infinite number of curves can be defined by the same asymptotes. However, these curves differ in shape, each curve described by a specific value of "G". Thus the description of a curve is unique when in addition to the position of its asymptotes, its shape is defined.

A family of capillary pressure curves have been computed based on the preceding equation and are shown as Figure 1. These curves can be utilized graphically to determine the characteristic parameters of any arbitrarily located curve. Those parameters that can be approximated from any capillary pressure curve are:

(1) Total interconnected pore volume,

(2) Extrapolated displacement pressure, and

(3) Pore geometry factor.

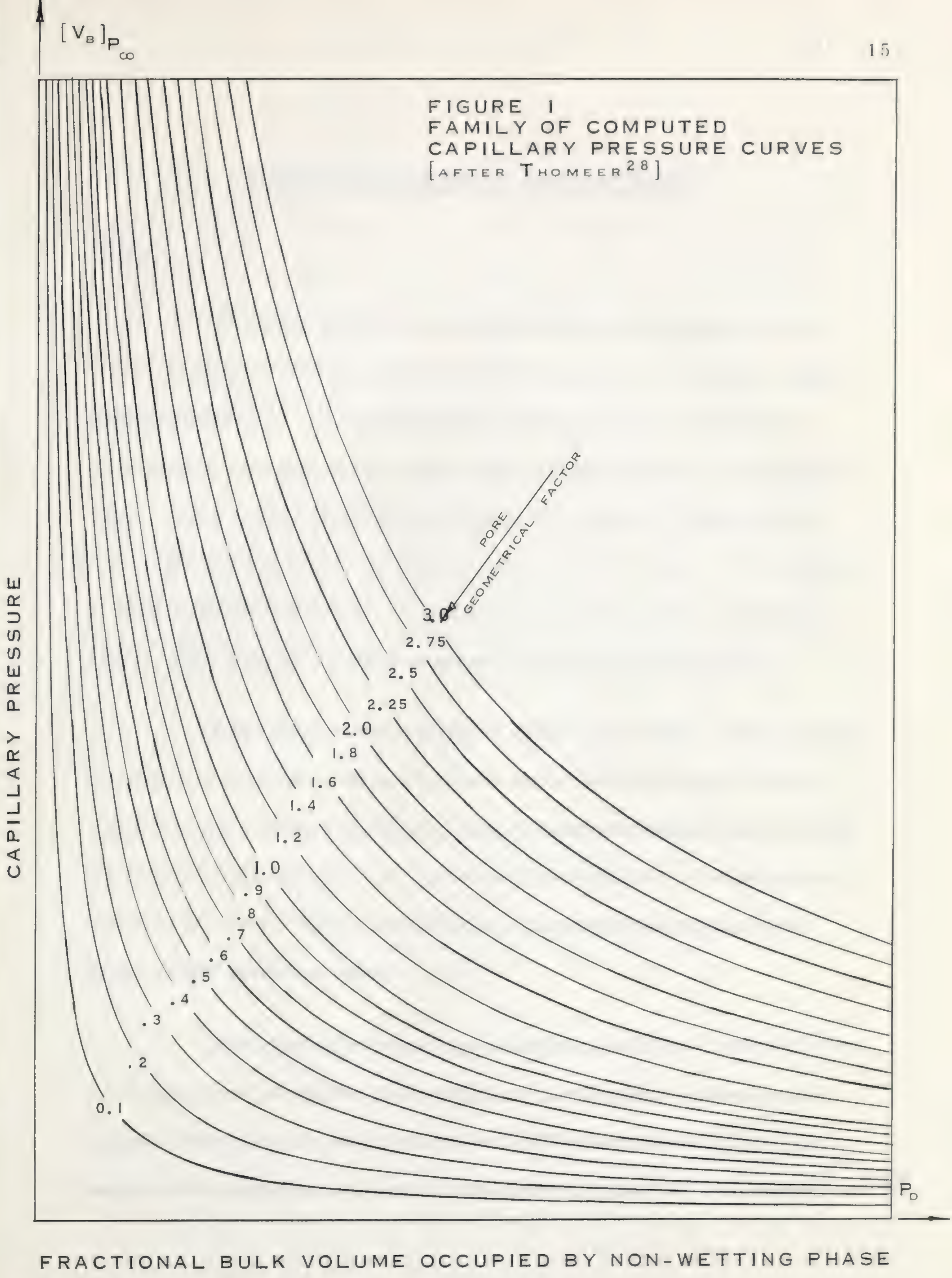

FIGURE I
FAMILY OF COMPUTED
CAPILLARY PRESSURE CURVES
[AFTER THOMEER[28]]

PROPERTIES OF BRINE AND BACTERIA

Brine

The fluid used throughout this study was an aqueous solution of sodium chloride, containing 25,000 parts per million by weight. Past experience(11,21) indicated that swelling of clays occurred in consolidated sandstones while determining permeabilities with distilled water. This caused erroneous permeability results by reducing the size of the fluid conductivity pores within the porous rock. The addition of salts to fresh water will, in many cases, eliminate this swelling of clays. This was the intended purpose in using the brine solution.

Limestone cores were also used in this work. Since calcium carbonate is relatively soluble in fresh water, the flushing of distilled water through a porous carbonate tends to leach or dissolve the walls of the pores. This results in an increase in permeability. This leaching action may be retarded by employing a saturated brine solution for permeability measurements.

A viscosity test was run on the brine solution used at 100° F., the temperature at which all permeability and plugging tests were conducted. The viscosity was found to be 0.7241 centipoises. This compares with a calculated viscosity of the brine solution of 0.72 centipoises(18)

and a viscosity of 0.6841 centipoises(22) for distilled water at the same temperature. As the pressure effect on viscosity of water is negligible for all practical purposes(18), the viscosity run on the brine at atmospheric pressure and 100° F. was assumed to be sufficiently accurate.

Bacteria

The effective pore radius of various oil producing rocks ranges from approximately one half to fifteen microns(10). In examining bacteria it is found that they frequently have dimensions that come within this same range. At least a dozen different types of bacteria are usually found associated with waterflood projects. It is not surprising that injection water containing excess bacteria can usually be considered to present a very serious formation plugging problem. A study(20) of 267 samples of injection water taken from various injection wellheads in Alberta indicated that 67 per cent of them were positive for various groups of micro-organisms which may have a deleterious effect on the petroliferous formation.

There is ample evidence in literature(2, 3, 15, 19) to indicate that bacteria in water will plug porous formations. However, the experimental conditions under which the results were obtained were generally different from field conditions, particularly with respect

to type and concentration of bacteria and injection pressures. A recent study(8) of six water injection systems in Texas and Oklahoma indicated that all six systems had heavy microbial contamination. However, by inclusion of other possibilities, only one appeared to be experiencing formation plugging troubles in which bacteria played the major role. There is some question of the relative importance of various types of bacteria as plugging agents in field injection systems(32).

The aerobic micro-organism Bacillus subtilis was used in this work. It is often found in copious quantities in field injection systems(20, 8). This organism is characterized by its rod shape. It has a uniform average size of four microns in length and one micron in diameter. It is spore forming and as such is very resistant to chemical methods of treating of injection water. In addition, the spores are resistant to temperature elevation such as occurs at the bottom of injection wells. When not producing spores it tends to grow in chains. Masses of these chains can augment the plugging of the formation. The growth of this organism is frequently accompanied by slime formation. The organism itself is of the same general size as the majority of bacteria commonly found in injection waters(15).

Initially, live bacteria were used; however, difficulties were encountered in controlling a constant concentration count during

a plugging run. Cores plugged with live bacteria were not used in the data tables in this study. As it was necessary to maintain constant concentrations with respect to time to obtain reliable information, all the data herein is based on plugging with bacteria that were killed using an autoclave method.

The constant bacteria concentration used was 3×10^7 per millilitre. A viscosity run of the bacteria in brine at 100° F. showed it had an identical kinematic viscosity with that of the brine alone of 0.7172 centistokes. However, the density of the bacteria in brine mixture exceeded that of the brine solution by 0.0011 gms/cc. The absolute viscosity of the mixture was 0.7253 centipoises at 100° F. However, considering the significant accuracy of other figures in this study, both the brine and bacteria-brine solution were considered to have a viscosity of 0.725 centipoises.

The specific gravity of the dead Bacillus subtilis microorganism is larger than that of the brine solution used. Over a period of six to eight hours the bacteria bodies would start to settle out of the suspension to the bottom of the container unless some mixing were present. In order to prevent this settling and to try to assure a completely homogenous mixture of bacteria in brine, the suspension was continuously agitated using a magnetic stirrer apparatus.

EXPERIMENTAL APPARATUS

and

PROCEDURES

Rock Property Determinations

The core specimens used in this study were selected from four distinct texture types. The Berea sandstone is well known for its homogeneous character. The Cardium sandstone chosen was composed of less uniform sand grains than the Berea but was considered to be a clean, well-sorted rock type. The Devonian cores were a completely heterogeneous type. From one centimetre to the next they ranged from completely dense matrix, with only very minor intercrystalline porosity, to pinpoint porosity with some streaks of oolites, to fine vuggy porosity with small hairline fractures up to one centimetre in length. The Indiana limestone cores were basically composed of oolitic porosity with secondary small vuggy and pinpoint porosity.

All cores were cut with a 2.5 centimetre interior diameter core barrel using water, at right angles to the main axis of 3 1/2 inch standard oilfield cores. This was done to assure that the core samples used had their main axis generally parallel to any bedding planes that may have been present in the cored formations. Both the Devonian and the Cardium cores were from Alberta oilfields, i.e., Swan Hills

and Pembina respectively. The Berea and Indiana cores were cut from surface outcrops. The cores were marked with an initial number to indicate the core type and a second number merely for identification purposes.

The cores were faced down to a fairly uniform size of approximately 8.5 centimetres in length. The residue fluids from each core were extracted using pentane. Extraction was continued until the dry weight of a core remained constant between successive runs. Bulk volumes were determined by the mercury displacement method. The porosity of each of the clean dry cores was then determined by the saturation method after the cores had been evacuated and saturated with distilled water.

Static capillary pressure vs. saturation data using air displacing brine, employing the porous diaphragm method were then obtained for most of the cores. The porous diaphragms used had extremely small pores that would not allow the non-wetting phase fluid, air, to enter it at pressures less than 100 centimetres of mercury. However, the porous membrane, being preferentially water-wet would allow the wetting phase fluid, brine, to be displaced through it and to be collected in a calibrated cylinder. The stepwise experimental procedure involved was originally proposed in 1947 and produces a curve

of capillary pressure versus water saturation. It has been adequately covered in literature; one of its best descriptions is by Rose and Bruce(26).

To check the results of the capillary pressure data by the desaturation method, a number of mercury injection capillary pressure curves for each sample type were run. This method is similar in principle to the preceding one except that mercury is injected into a completely evacuated sample. Pressure was applied incrementally as before, with the mercury volume injected into the rock pore being noted at each pressure. A curve of capillary pressure versus mercury saturation is thus obtained. This procedure was initially proposed by Purcell(24). It has a definite advantage of speed over the previous method; however, any sample used is ruined for subsequent testing.

Wettability imbibition tests were run on several samples of each type as outlined by Bobek et al(4). To test for water wettability, the cores were evacuated and saturated with a light oil of 1.5 centipoise viscosity. They were then placed in the imbibition cell and the cell was filled with brine. A plot of time versus per cent of pore volume imbibed by the brine was the result. The oil was displaced out of the core by the water and rose into the calibrated cylinder at the top of the cell where it was measured as the per cent of pore volume imbibed by the water.

To test for oil wettability, a similar run was conducted. The cores were evacuated and saturated with brine and then placed in the imbibition cell. The imbibition cell was inverted and filled with the light oil. Any water that was displaced out of the core by the oil could settle down into the calibrated cylinder where it could be measured as the per cent of pore volume imbibed by the oil.

Permeability, Plugging and Backwashing

A schematic sketch of the apparatus utilized for permeability determination of the cores, plugging and backwashing is shown on Figure 2. All pressure lines in the system were constructed of 1/8 inch stainless steel tubing with autoclave fittings and valves.

All the cores to be plugged were mounted in 1 1/2 inch extra heavy API line pipe. The annular space between the pipe and the core was sealed with an epoxy resin. A continuous bond between the core and the resin and between the resin and the pipe was thereby obtained. This insured that there was no bypassing of fluids past the cores. The ends of the cores were cut and ground flush with the end of the pipe, which had been cut to an overall length of eight centimetres. Care was taken to try not to contaminate the ends of the core. Three pressure taps were drilled along the core at two centimetre

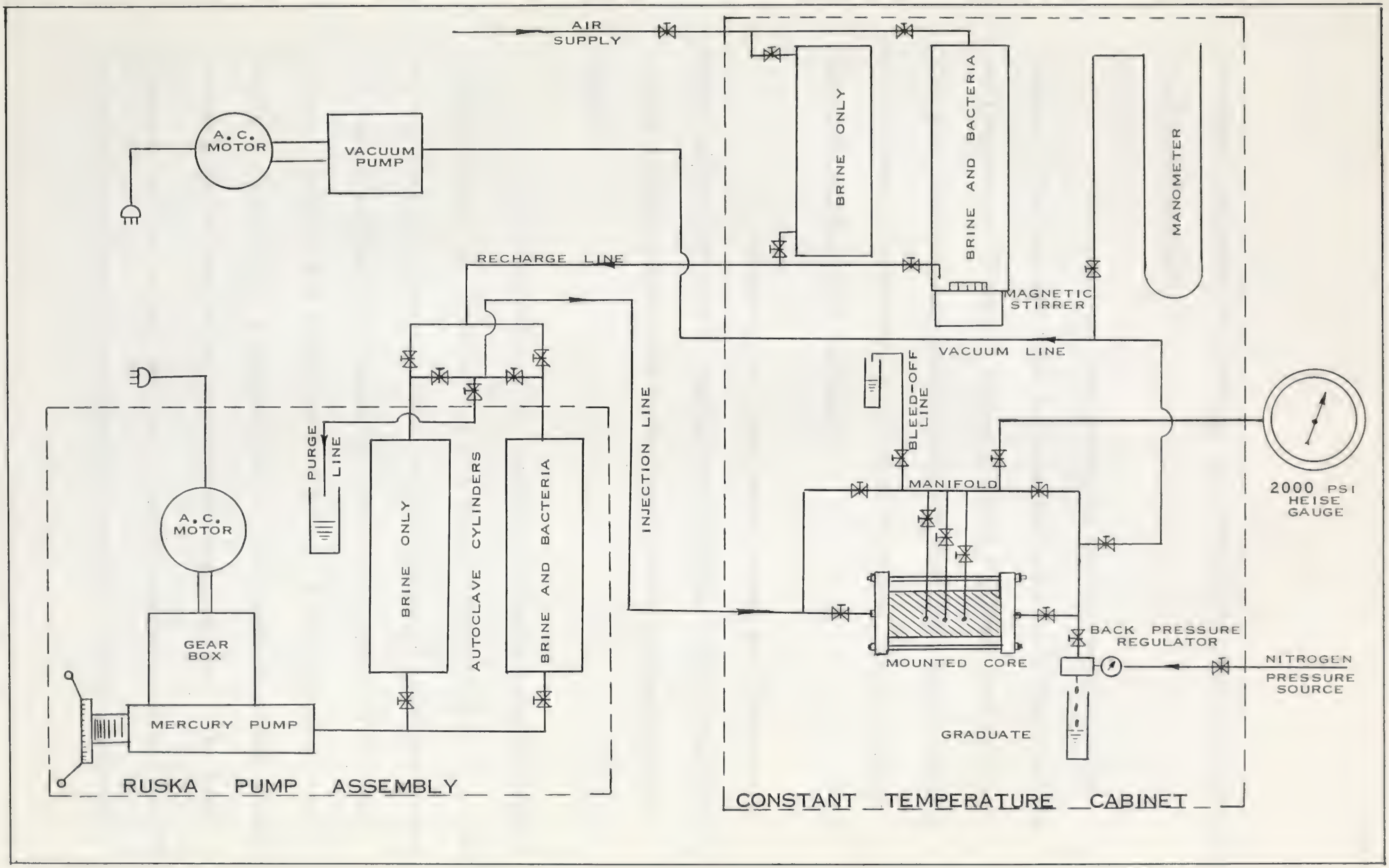

FIGURE 2. SCHEMATIC SKETCH OF PLUGGING APPARATUS

intervals. Seals for the pressure taps were made in the epoxy resin filler with "o-rings".

The core was then assembled between two brass end flanges. The seal was made between the epoxy resin filler and the end flanges with "o-rings" larger in inside diameter than the core. This was done to ensure that injected fluids would be in full contact with the entire cross-sectional area of the core. The end flanges were held together with tie-rods.

All equipment and lines were cleaned and flushed with methyl alcohol initially so that any live bacteria in the system were completely eliminated. The bacteria and brine container was autoclaved.

A Ruska constant volume displacement pump was used for injection purposes. This pump was a double-cylinder type. One cylinder was used for brine, the other for the bacteria in brine suspension. The pump was geared for discharge rates of from 10 to 1200 cc per hour per cylinder and calibrated to 0.01 cc. A Grove back pressure regulator, supplied by a nitrogen bottle, was used to maintain a back pressure on the core during all fluid displacement runs. The back pressure was varied with each core type so that during all tests on the cores the inlet pressure was kept high enough to simulate reservoir

conditions. A constant temperature air bath cabinet was employed at 100^{o} F. throughout all the runs to ensure no temperature variation during any given test. A Heise pressure gauge with a range of 0 to 2000 psig was used through the manifold system for all pressure measurements.

The rate for determining permeability and for plugging was selected at 500 cc per hour. This rate is equivalent to a field injection rate of approximately 30 barrels per day per foot of net pay in an 8 1/2 inch hole.

The cores were evacuated overnight, using a vacuum pump, in preparation for saturation with brine the next morning. Following the saturation of the core a stabilized pressure profile had to be established to determine the liquid permeability. In testing many cores, it was noted while establishing the permeability profile, that the pressure gradients in the inlet and outlet end section were higher than might be expected. This phenomena was probably due to small rock particles left in the core ends as a result of cutting and grinding. It was impossible to remove them by brushing or air blowing. However, after about 10 to 20 pore volumes were injected through the core, the outlet end pressure difference was always reduced. The small rock particles at the outlet end had been flushed out. The core and holder were turned end to end and the procedure repeated.

Normally during any run the gauge was left on reading the inlet pressure. To take a full reading of pressure profiles throughout the core, the inlet manifold valve was closed and the gauge and manifold pressure bled off through the bleed line to a pressure below that set on the back pressure regulator. The bleed-off valve was closed and the outlet manifold valve opened and its pressure checked on the gauge and the valve closed. The pressure tap valve adjacent to the outflow end was open and its pressure read from the gauge. This stepwise procedure was repeated up the core to the inflow end manifold valve.

After a stabilized pressure profile was satisfactorily established through the core, over a 15 minute period, the lines were displaced to the bacteria and brine mixture. The cylinder and barrel containing this mixture were placed in operation and plugging of the core was commenced. Pressure profiles through the core were read, as described, at regular fluid production increments. These volumes were then converted to pore volumes injected. Plugging runs continued until permeability was reduced to at least 30 per cent of the initial permeability.

At the end of the plugging test, the injection lines were purged with brine to remove any bacteria present. The core and holder were turned end to end so that backwashing could commence. In all

cases, except for the Indiana cores, backwashing rates were conducted at 1200 cc per hour, a 2.4 fold increase over plugging rate. Again, this was done to simulate field conditions. The rate for backwashing the less permeable Indiana cores was 500 cc per hour because the range of the Heise gauge limited injection pressures to 2000 psig. Backwashing continued until 88 to 90 per cent of initial permeability was restored in the test core.

DISCUSSION OF RESULTS

Capillary Pressure Curves

Capillary pressure curves using an air-brine desaturation method were obtained for various cores of the four types included in this study. The capillary pressure versus saturation results were converted to capillary pressure versus fractional bulk volume occupied by the non-wetting phase fluid and plotted on a 2 x 3 cycle log-log scale. Typical curves of the four rock types considered are shown in Figures 3, 4, 5 and 6 on the following pages.

Prior knowledge of the effective porosity of the cores was useful in determining each pore geometry factor "G". The ordinate axis of the family of curves shown on Figure 1 was made to exactly under-lay the value of effective porosity of the core expressed as a fraction. The plotted experimental points were moved vertically over the family of curves until the best-fitting curve was found. The value of "G" was read from the family curve and applied to the experimental points and the curve drawn. For the multi-porosity cores it was necessary to approximate the value of the effective porosity of each pore system. Then, the ordinate axis of the family of curves was made coincident with this approximated porosity fraction. A similar procedure was followed as described above for each pore system.

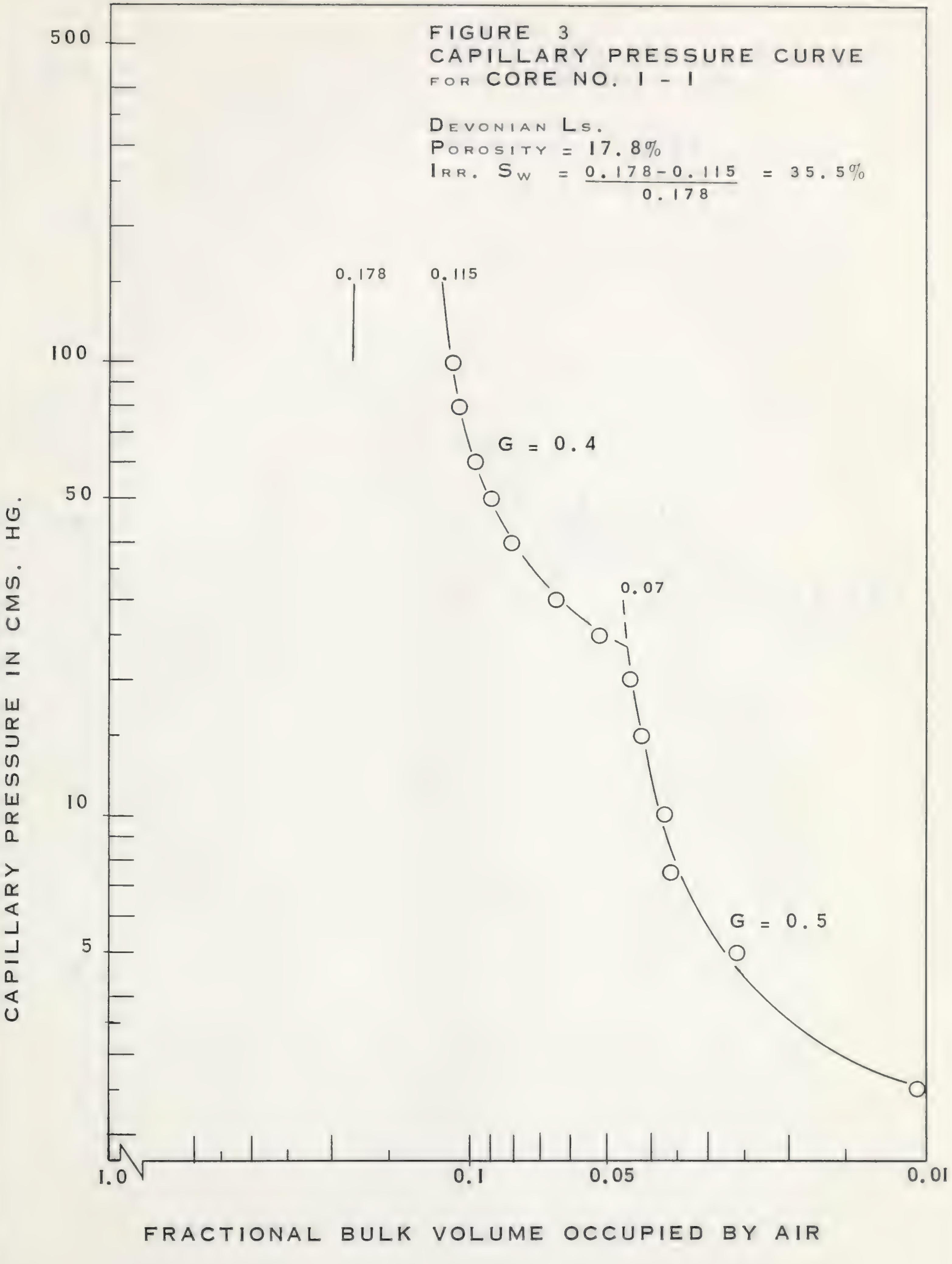

FIGURE 3
CAPILLARY PRESSURE CURVE
FOR CORE NO. 1 - 1

Devonian Ls.
Porosity = 17.8%
Irr. $S_W = \frac{0.178-0.115}{0.178} = 35.5\%$

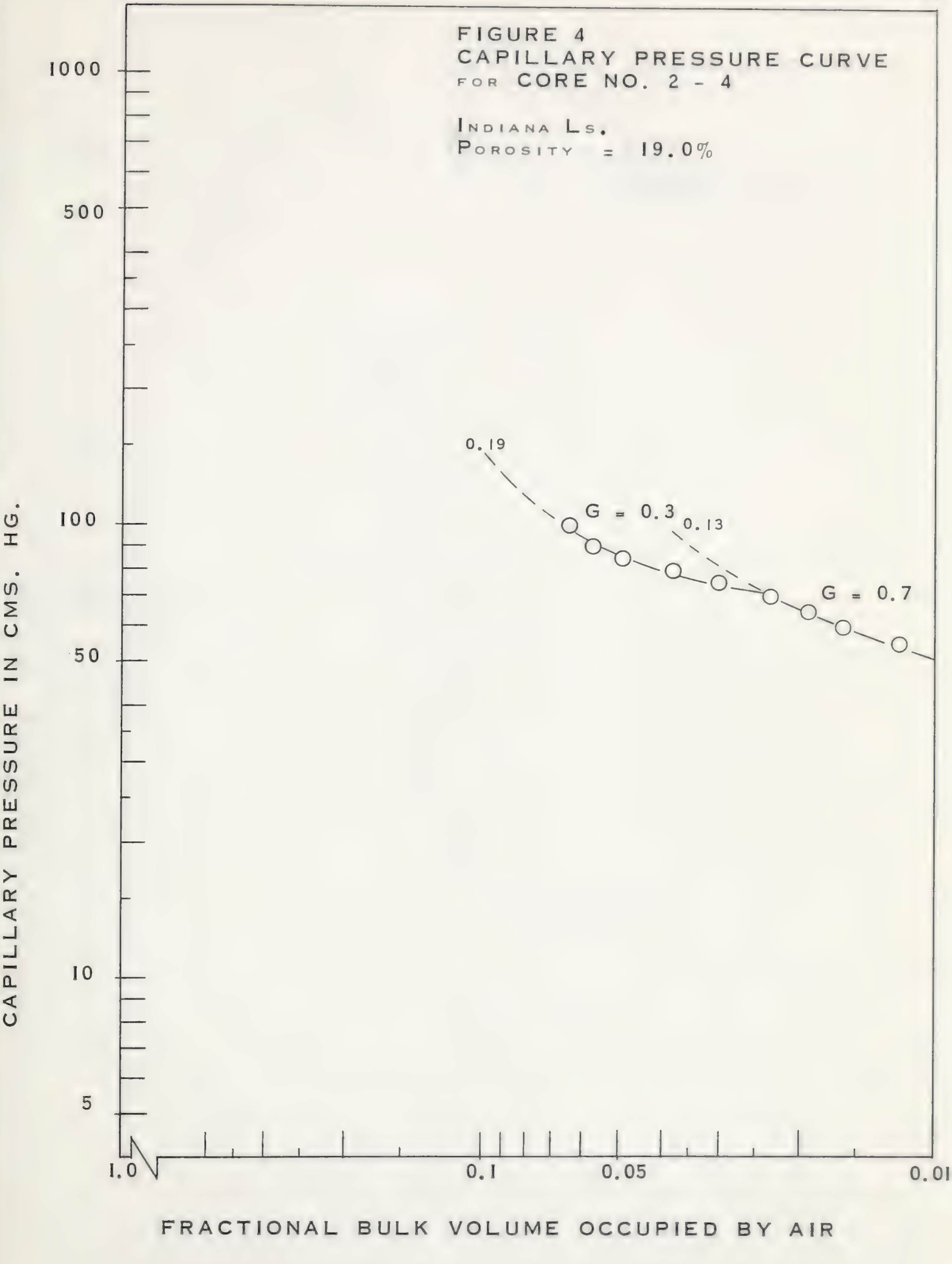

FIGURE 4
CAPILLARY PRESSURE CURVE
FOR CORE NO. 2 - 4

INDIANA LS.
POROSITY = 19.0%

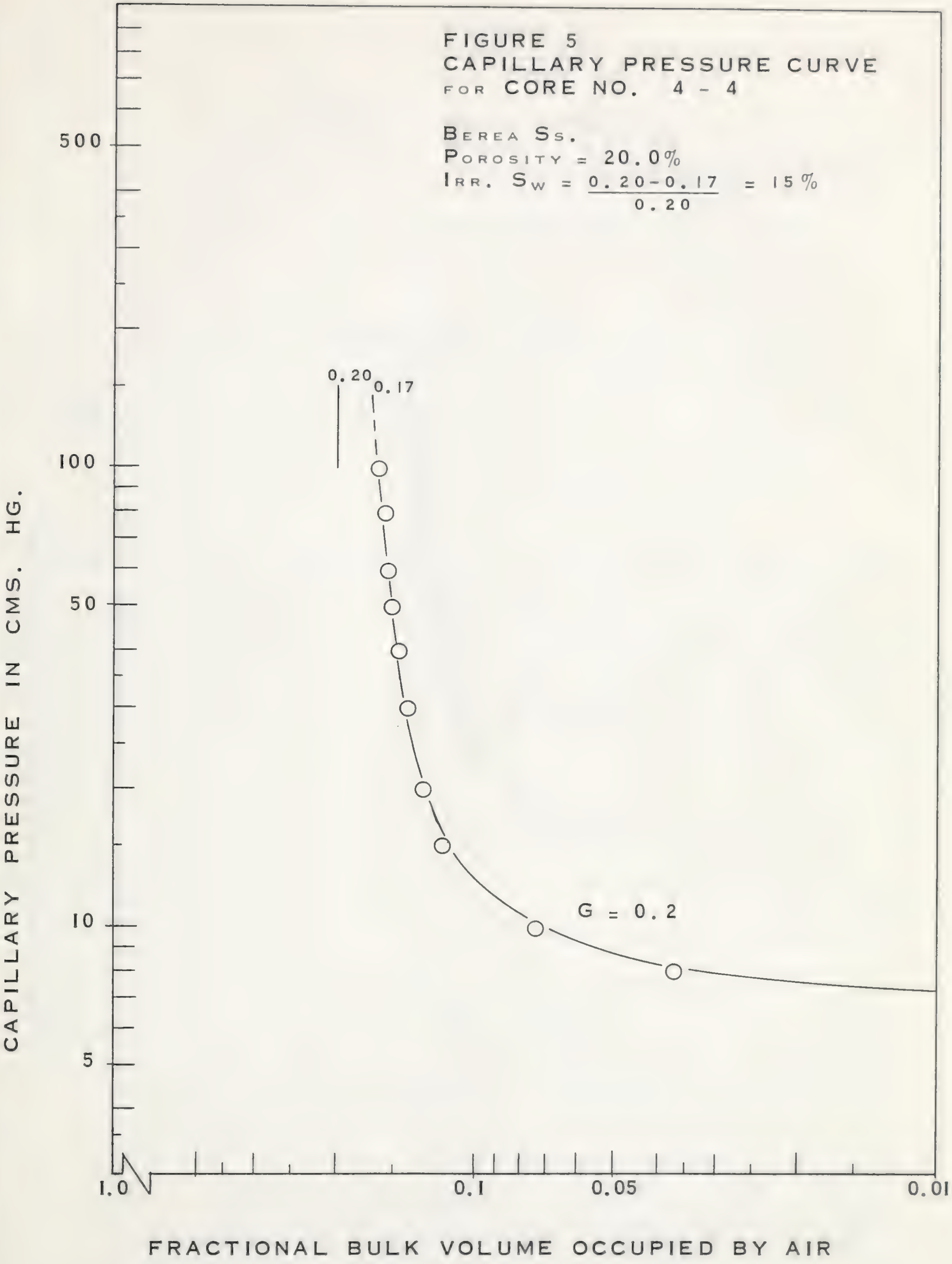

FIGURE 5
CAPILLARY PRESSURE CURVE
FOR CORE NO. 4 - 4

BEREA SS.
POROSITY = 20.0%
IRR. $S_W = \frac{0.20-0.17}{0.20} = 15\%$

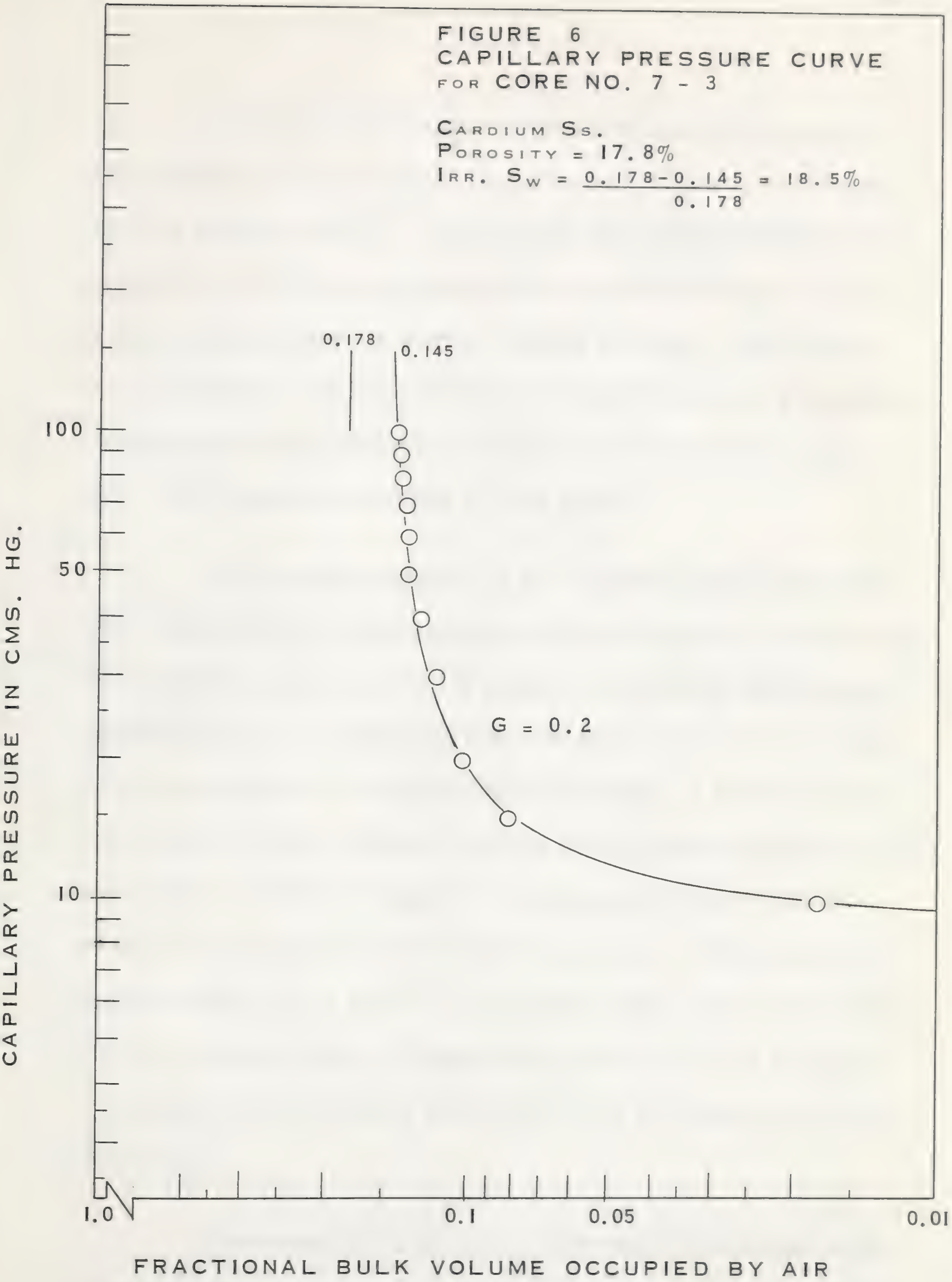

FIGURE 6
CAPILLARY PRESSURE CURVE
FOR CORE NO. 7 - 3

CARDIUM SS.
POROSITY = 17.8%
IRR. $S_W = \frac{0.178 - 0.145}{0.178} = 18.5\%$

Irreducible water saturation was determined from most of the capillary pressure curves by the method originally outlined by Thornton and Marshall(29). In this study, this method involved extrapolating the curve to the appropriate fractional bulk volume occupied by the non-wetting fluid at infinite capillary pressure. As the effective core porosity was already known and could be verified graphically, a simple calculation yielded the irreducible water saturation in per cent. This calculation is shown on each graph.

The entrance pressure of air into the tightest porous porcelain discs used in the capillary pressure apparatus was approximately 120 centimetres of mercury (23.2 psig). Unfortunately, this was not sufficiently high to allow the capillary pressure curves for the Indiana cores to approach an irreducible water saturation. A number of mercury injection capillary pressure curves were obtained on Indiana cores. One of these is shown on Figure 7. It indicates that the irreducible non-wetting phase saturation would be 24 per cent. This agrees satisfactorily with previous work(16) correlating connate water with permeability for carbonate cores. Consequently, 24 per cent was the figure used as the irreducible water saturation for all the Indiana cores that were plugged.

The shape character of the carbonate Devonian and Indiana curves is extremely interesting. The interpretation curves given to the

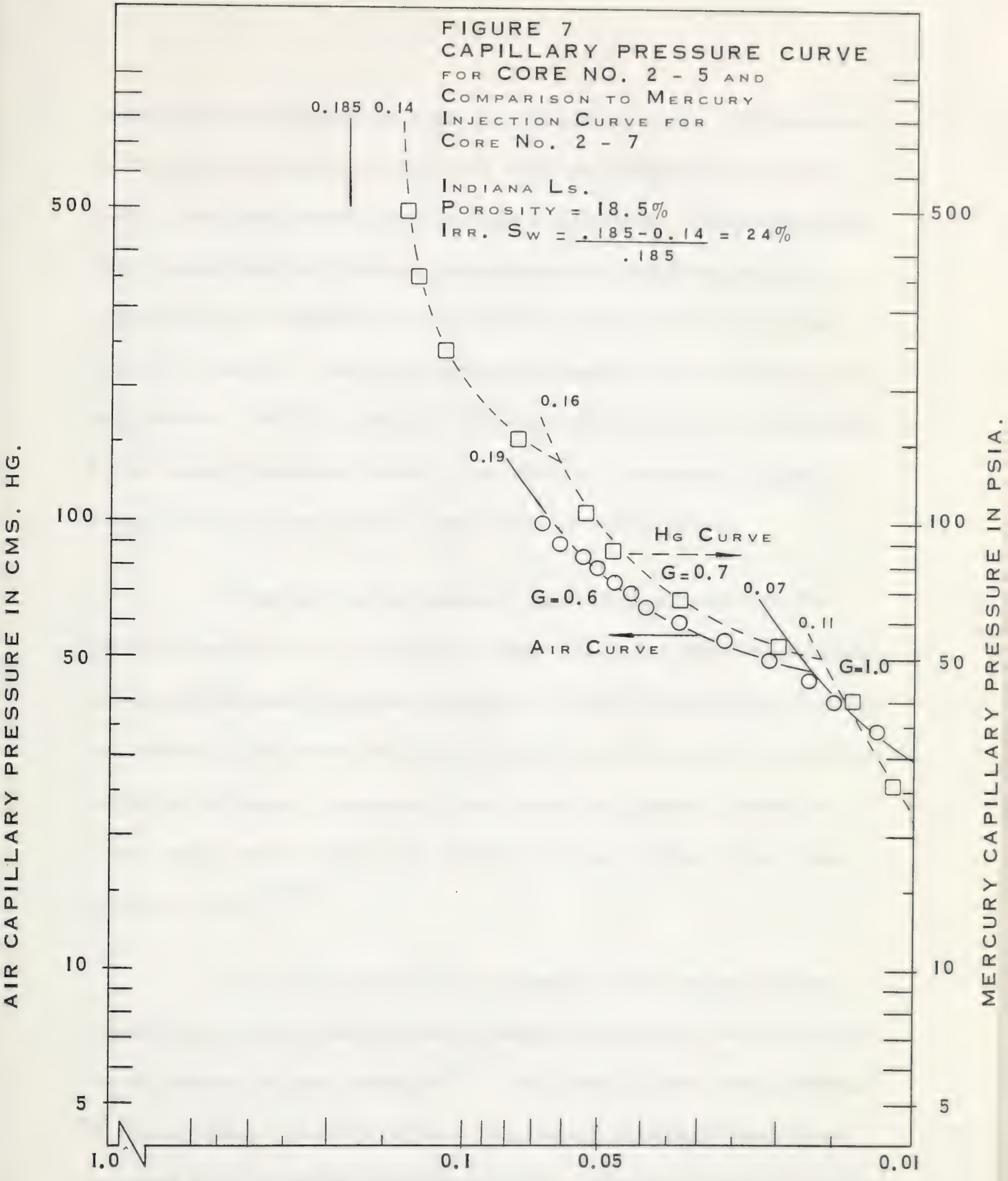

FIGURE 7
CAPILLARY PRESSURE CURVE
FOR CORE NO. 2 - 5 AND
COMPARISON TO MERCURY
INJECTION CURVE FOR
CORE NO. 2 - 7

INDIANA LS.
POROSITY = 18.5%
IRR. $S_W = \frac{.185-0.14}{.185} = 24\%$

experimental points may be open for some discussion. For example, the double curve shown on Figure 3 could be replaced by a single curve, positioned through an average of the points. This would indicate a single porosity system with an excess number of pores of radius size corresponding to the pressures where the curve bulges to the left. However, this core appeared visually to have a double porosity system. One is a primary intercrystalline porosity represented by the higher-pressure curve. The other is a secondary slightly vuggy porosity represented by the lower-pressure curve.

Physical rock properties, depending primarily on the larger pores of a core sample, are expected to be related to the parameters of the lower-pressure capillary curve in a double pore system. For example, the contribution to permeability of the finer pores represented by the upper-pressure curve, shown on Figure 3, would be minor compared to that by the relatively larger pores, of the lower-pressure curve(28).

It is not uncommon for carbonate rocks having induced porosity and a very complex pore configuration system to have two or more systems of pore openings(1). Their basic matrix rock material is usually finely intercrystalline. It contains uniformly small pore openings which comprise one pore system. One or more systems of larger openings usually occur as a result of leaching or fracturing

the primary rock material. This multi-pore system is evident through the capillary pressure curves of all the carbonate cores studied herein. However, both the Berea and Cardium sandstone core types indicate a uniform single porosity system through their capillary pressure curve characters.

The mercury injection capillary pressure curves can be compared to the desaturation capillary pressure curves by applying an appropriate correction factor$^{(24)}$.

$$\frac{P_c\ hg}{P_{cw}} = \frac{\sigma\ hg\ \ \mathrm{Cos}\ \theta\ hg}{\sigma\ w\ \ \mathrm{Cos}\ \theta_w} \approx 5.$$

Where: $P_c\ hg$ = mercury injection capillary pressure in psia.

P_{cw} = air-water desaturation capillary pressure in psia.

$\sigma\ hg$ = 480 dynes/cm.

$\sigma\ w$ = 70 dynes/cm.

θ_w = 0^o.

θ_{hg} = 140^o.

The above conditions are for fully water-wet rocks which are not always the case. A study$^{(31)}$ of these two methods of determining capillary pressure curves indicated that for limestone cores the conversion factor could range from 5.25 to 10.1, depending on rock surface properties.

Comparison conversion factor used in this study was 5.17, the appropriate factor to change centimetres of mercury to pounds per

square inch. It was selected as a convenient figure for graph purposes. Figure 7 and Figures 22, 26 and 27 in the Appendix, illustrate the comparison between the two methods. The general curve shape similarities are quite uniform, considering that each figure shows curves from two different cores.

Effects of Wettability

The rate and volume of spontaneous imbibition of the wetting phase by a porous rock is a reliable test for semi-quantitative determination of preferential rock wettability(4). Imbibition tests indicated that two core types, Indiana and Berea, had definite preferentially water-wet characteristics. A plot of the results of the imbibition tests for typical Indiana and Berea cores is shown on Figure 8.

Imbibition tests for both preferential water wettability and preferential oil wettability were conducted on the Devonian and Cardium cores. These tests indicated these cores were of neutral or indefinable preferential wettability. That is, when saturated with water they would not imbibe oil over a two hour period and when saturated with oil they did not imbibe water over the same time period. It is believed that these local oilfield cores were cut using an oil-base mud. This could have altered their preferential wettability making them less water-wet than the actual reservoir(4).

FIGURE 8 IMBIBITION CURVES FOR WATER-WET CORES

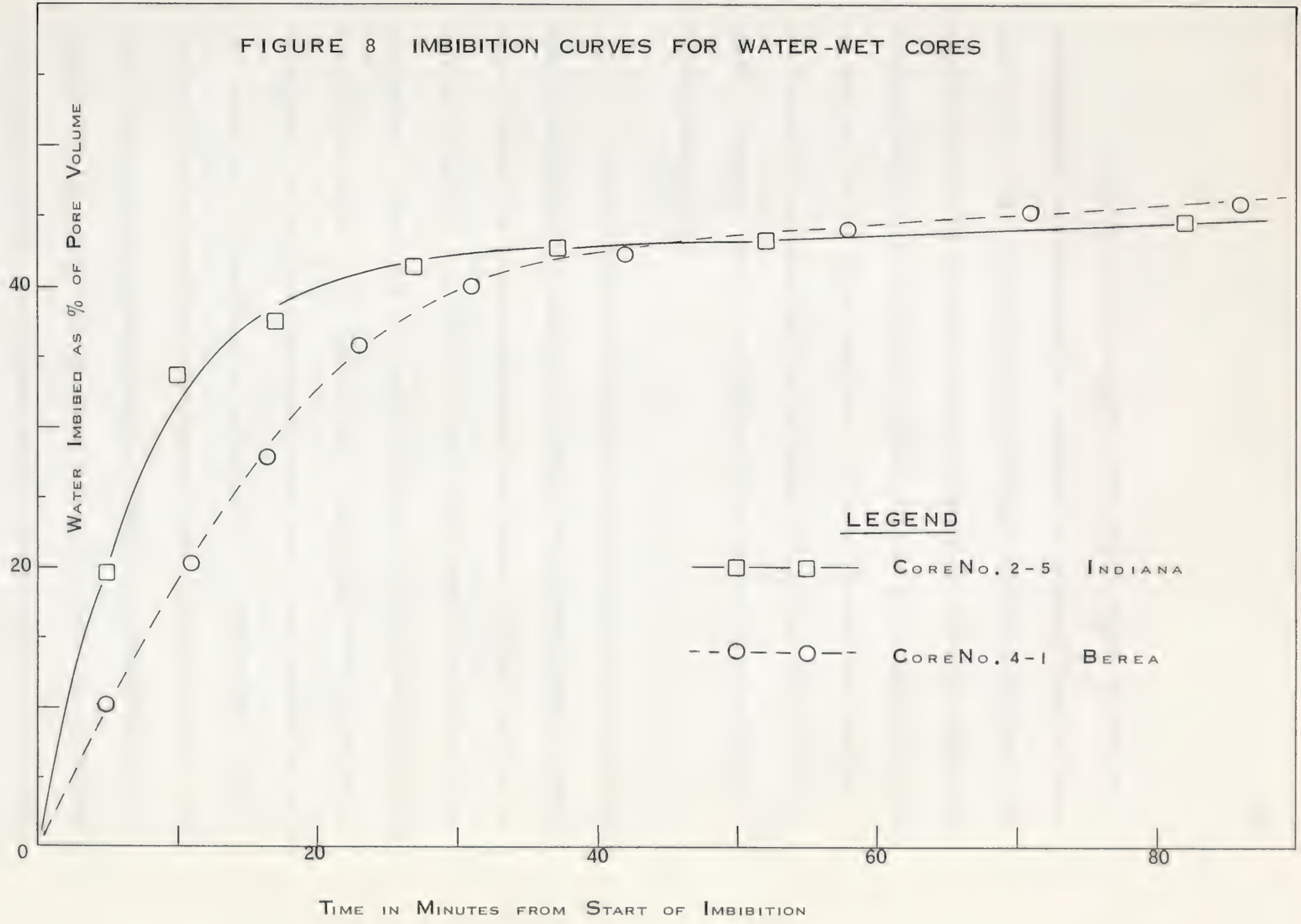

The imbibition tests indicated only a degree of relative wettability and are dependent on a number of factors. Some of these factors are: rate of imbibition, the strength and activity of the compounds adsorbed by the rock surface which largely control wettability, the shape and size of the porous media sample, its permeability, and the viscosity of the fluids involved. Calhoun(7) concluded that the imbibition of the displacing fluid indicated relative wettability to this phase. However, lack of imbibition did not indicate non-wetting by the displacing phase.

An examination of the capillary pressure curves on Figures 3 and 6 for typical Devonian and Cardium cores shows that an actual neutral wettability is impossible for these cores. If they truly had a neutral wettability, the cosine of the contact angle θ, which would be 90 degrees, is zero and the capillary pressure curves would not have occurred as shown. Further, if the contact angle were approaching 90 degrees, the capillary pressure curve would rise normally to a certain value, until it overcame all surface forces, then become almost horizontal as the saturation was reduced to the irreducible with a very minor amount of increased pressure. This curve characteristic is evident from Figure 6, the Cardium core. However, this sandstone is quite regular and the curve shape may be affected just as much by the porous media regularity as by its contact angle. On the basis of the

evidence available, it can be stated that all core types included in this study were preferentially water-wet to some degree. The Devonian and Cardium cores did not have a sufficiently strong water-wet characteristic to indicate this preferential wettability by means of an imbibition test.

Based on the above factors, the Indiana cores have the strongest preferential water-wettability character. This is evidenced by the rapid initial rate of imbibition, shown on Figure 8, despite the low permeability. A strong degree of preferential water-wettability was also indicated by the Berea cores as shown by their imbibition curve.

Next in degree of wettability are the Devonian cores. This is based on the steeply sloping capillary pressure curve which would indicate that the contact angle is not approaching 90 degrees and that their permeability is somewhat less than the Cardium cores. The Cardium cores showed the weakest preferential water-wettability tendency relative to the other cores used in this work.

Capillary pressure curves are very sensitive to the state of the internal surface of the porous media(27). This is due to the dependence of capillary pressure on surface tension and the contact angle or degree of preferential wettability. Thus, the degree of

preferential wettability will cause a general shift in a capillary pressure curve from that position it would occupy if it were completely water-wet. In order to be able to correlate effectively those rock properties indicated from the capillary pressure, it is necessary that each core type have the same degree of preferential wettability. This was not the case in this study, so a brief discussion concerning the effect of the degree of wettability on irreducible water saturation and the pore geometry factor "G" follows.

To start with a base, the Indiana cores were considered to have a contact angle of zero because they exhibited the strongest preferential water-wet ability. The values shown for the "G" factor and irreducible water saturation for Indiana cores are quite accurate. It has been observed that small deviations of the contact angle from zero only slightly displace the capillary pressure curve(26). This would apply to the Berea cores which have a contact angle only slightly greater than those of the Indiana cores. For the purposes of this report, those values associated with the Berea capillary pressure curves are considered to be sufficiently accurate.

However, both the Devonian and the Cardium cores have contact angles considerably greater than that of the Indiana cores. If these two core types had the same degree of preferential wettability as the Indiana cores, their capillary pressure curves would have been located at higher pressures and shifted to the right of the locations in

which they are shown. The exact amount of this change in position of the Devonian and Cardium curves is not known because the exact contact angles are not known. The result is that to correlate capillary pressure curve characteristics at the same degree of wettability, both the irreducible water saturation values and the "G" factor values as shown must be increased for the Devonian and Cardium cores.

Plugging Results

The pressure taps positioned at two centimetre intervals along the core sample, allowed an investigation of the plugging trend within the core. However, it was the total over all core permeability that was considered when calculating the permeability ratio, i. e., the ratio of reduced permeability to initial permeability.

The brine solution appeared to control effectively any matrix or clay swelling within the sandstone cores. No indication of reduction of permeability with time was noted while conducting the permeability determinations. Some minor pressure decreases were noted in the runs on Indiana limestone cores. This was probably due to the unsaturated brine solution dissolving some of the calcium carbonate rock and thereby increasing pore sizes. However, this pressure change had a negligible affect on the permeability calculations because of the high pressure drop through the Indiana cores.

During the course of this experimental work, twenty-six core samples were tested. However, due to the extremely heterogeneous core properties of some of the rock samples, the data of some of these were not considered satisfactory. The results of fifteen cores, considered to be the most accurate and representative, were selected to illustrate the plugging effect of bacteria on the rock types selected.

It was expected that the majority of the pressure drop due to plugging would occur at the input end of the core. This had been experienced by previous investigators(11,13,14,17). Typical representative plugging profile results are shown on Figures 9, 10, 11, and 12 on the following pages. It is extremely interesting to observe that the major part of the pressure drop was not confined, in all cases, to the input end of the core.

The majority of the plugging in the clean, homogeneous, uniform-grained, consolidated sandstones was located near the input end of the cores. The heterogeneous carbonate cores behaved more irregularly. Plugging was observed well within the core. These results indicated that depth of plugging within porous rock is a function of the pore geometry. The plugging profiles, Figures 9 to 12, showed an increase in plugging depth of penetration with an increase in the pore geometry factor "G".

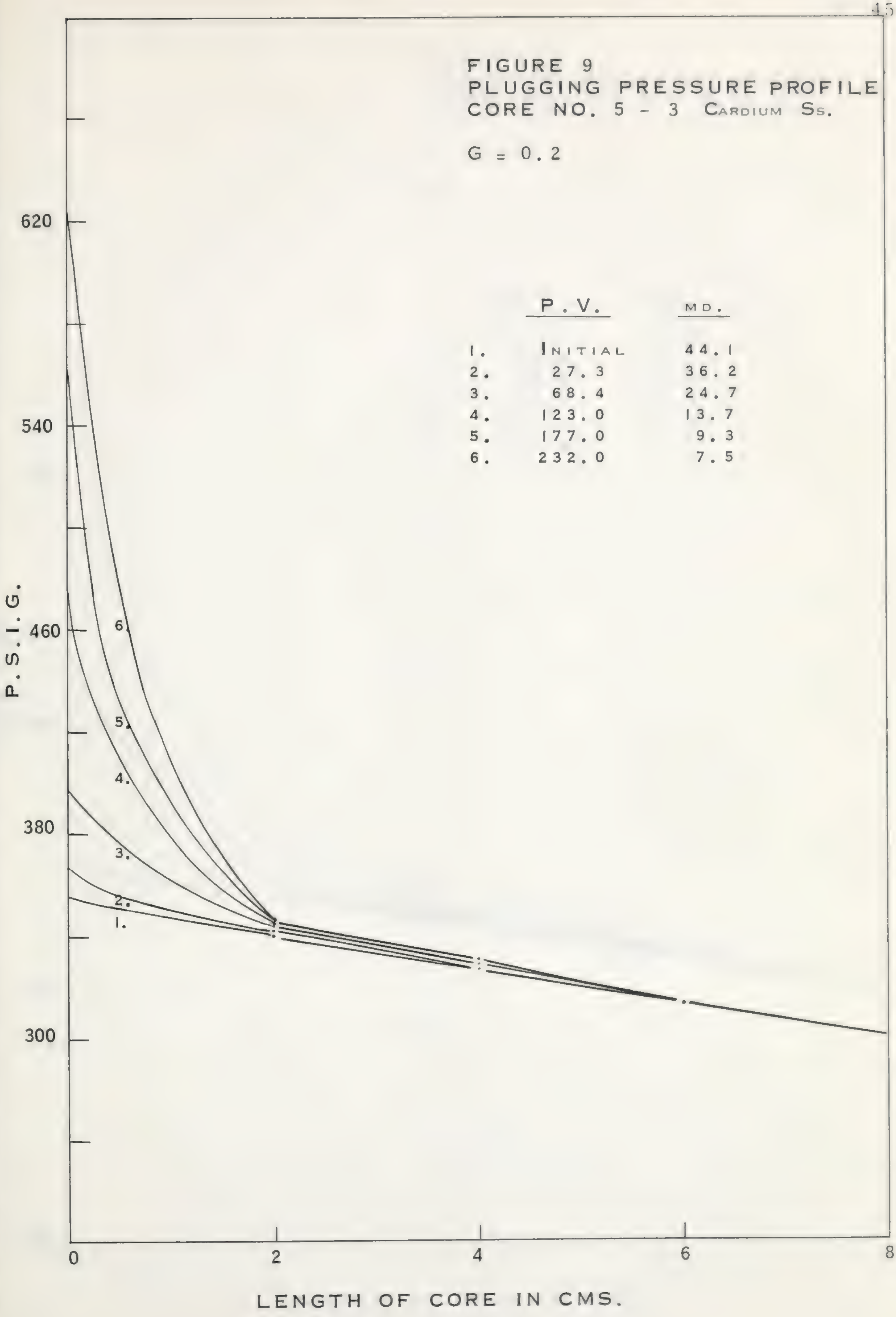

FIGURE 9
PLUGGING PRESSURE PROFILE
CORE NO. 5 - 3 CARDIUM SS.

G = 0.2

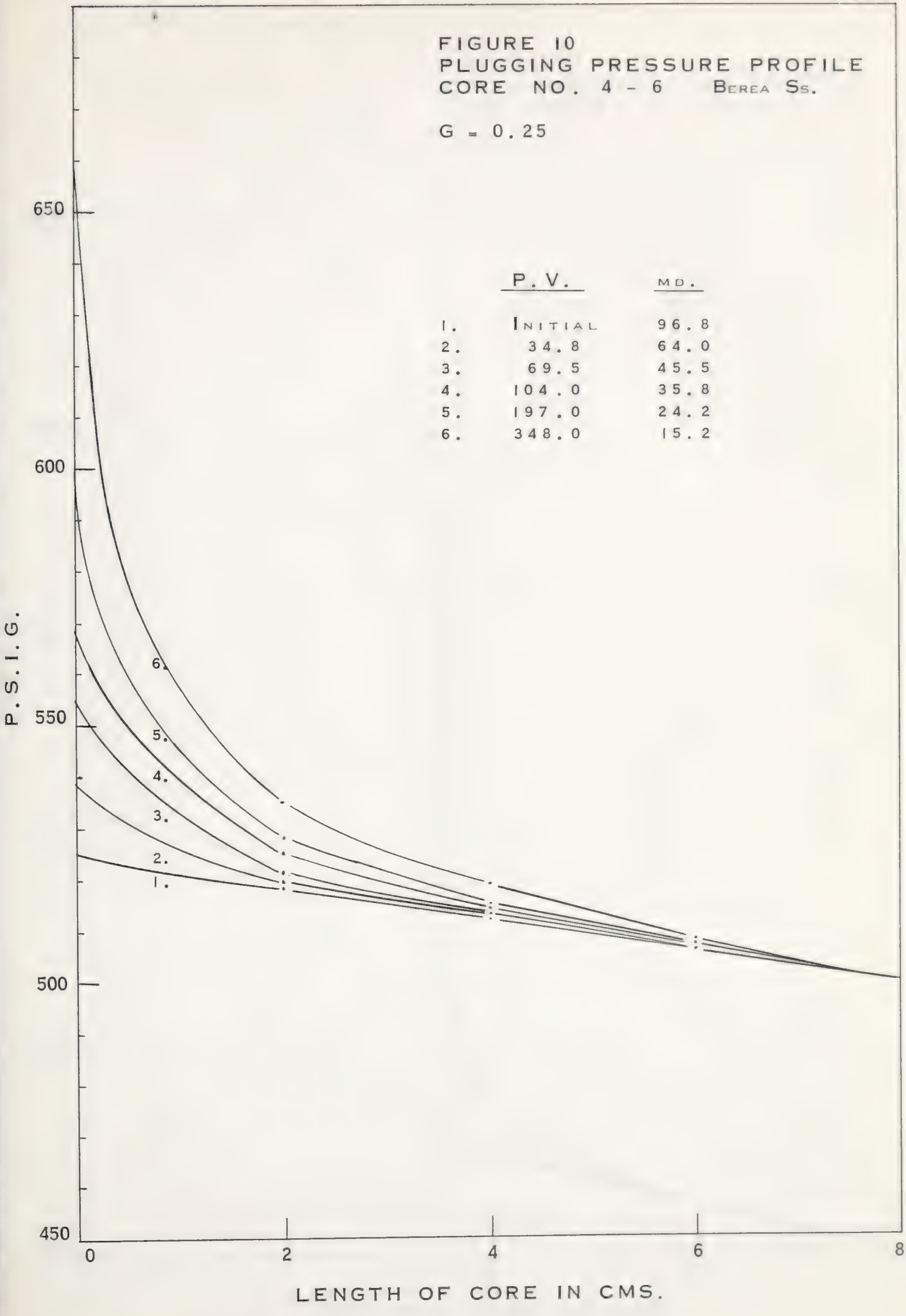

FIGURE 10
PLUGGING PRESSURE PROFILE
CORE NO. 4 - 6 Berea Ss.

G = 0.25

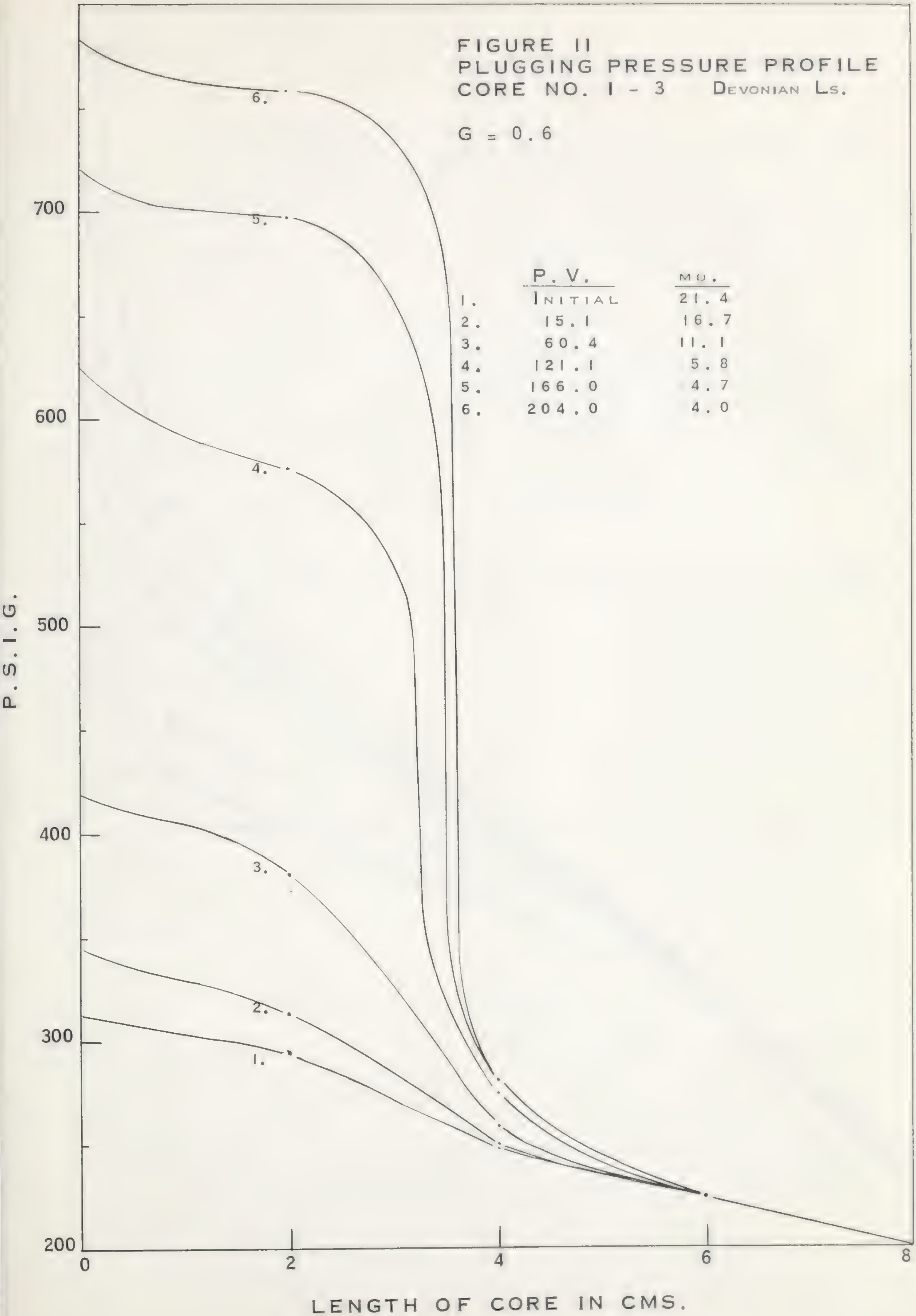

FIGURE II
PLUGGING PRESSURE PROFILE
CORE NO. I - 3 DEVONIAN LS.

G = 0.6

	P. V.	MD.
1.	INITIAL	21.4
2.	15.1	16.7
3.	60.4	11.1
4.	121.1	5.8
5.	166.0	4.7
6.	204.0	4.0

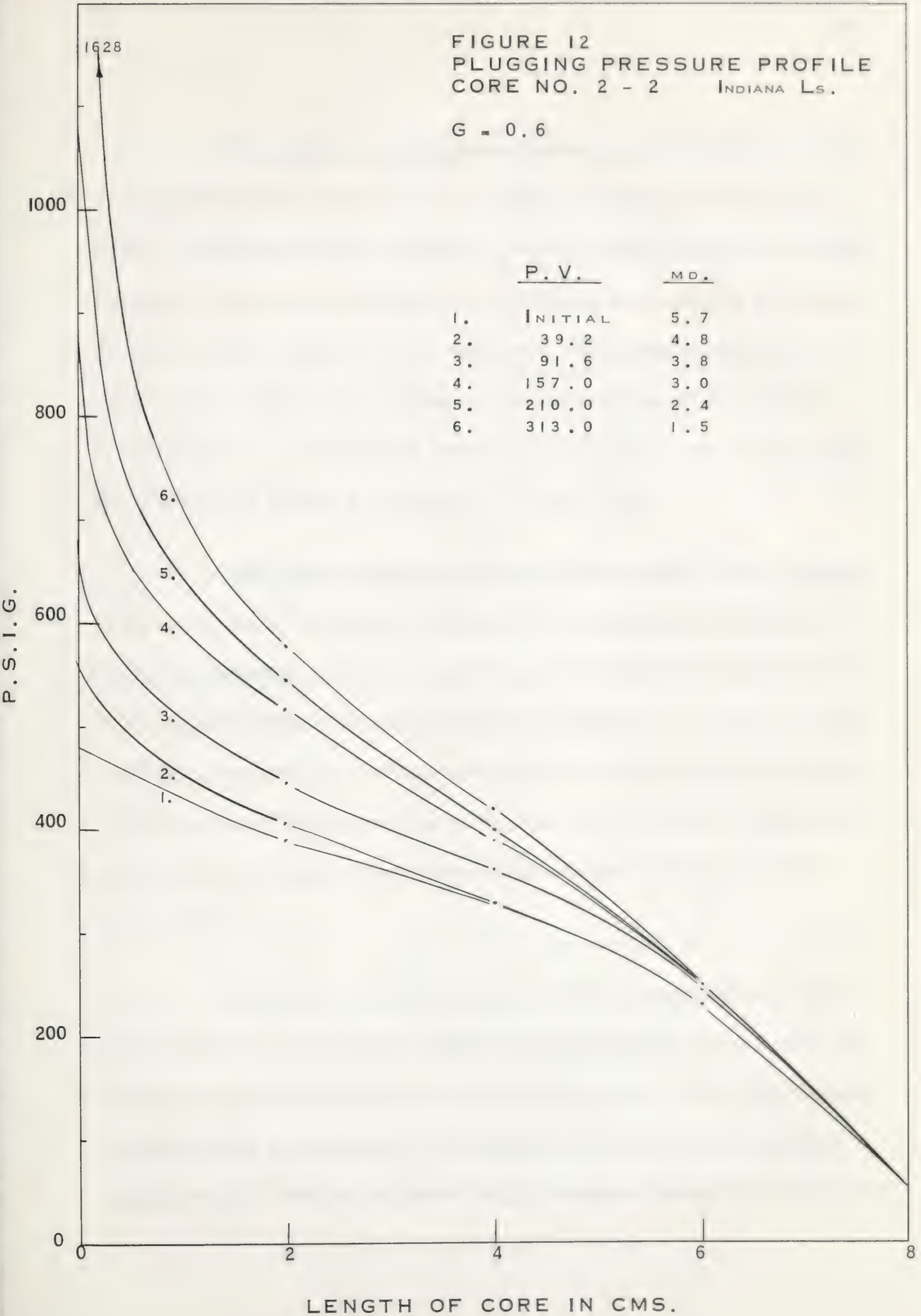

FIGURE 12
PLUGGING PRESSURE PROFILE
CORE NO. 2 - 2 INDIANA LS.

G = 0.6

	P.V.	MD.
1.	INITIAL	5.7
2.	39.2	4.8
3.	91.6	3.8
4.	157.0	3.0
5.	210.0	2.4
6.	313.0	1.5

The sandstones with homogeneous pore sizes did not allow much penetration into the core body before bridging of some of the pores was initiated by the bacteria. As most of the pores were within the same size range this initiation of plugging was confined to a narrow cylinder of core adjacent to the inlet face. Plugging progressed with the bacteria solids accumulating to completely plug off the initially bridged pores. The pressure profiles through the cores indicated that the majority of plugging remained in the inlet end.

The heterogeneous limestone cores showed some plugging at the input end. This was probably due to the small sized pores bridging and plugging near the inlet face. Most of the bacteria solids were carried within the larger sized pores into the core body until they reached a restriction. As the restrictions in the larger pore channels were disordered throughout the core, the pressure profile indicated a distribution of plugging away from the inlet face well back into the porous rock.

Figure 11 illustrates the progress of plugging in a heterogeneous system. The initial profile indicates that the first section of the core was more permeable than the next section. This was visually observed prior to mounting. The upstream section of the core was slightly oolitic, with some minor vuggy secondary porosity. This

was followed by a dense section with only intercrystalline porosity. This change from a relatively large pore system to a small pore system probably accounts for the severe plugging in this section of the core.

Some preliminary runs were made with live bacteria because it was a simple matter to check on the number of bacteria coming through the core. After approximately 100 pore volumes were injected through the core, some minor amounts of bacteria were noted in the effluent. However, toward the end of the tests, the concentration of bacteria coming out of the core was periodically greater than that going in. It would appear that some of the accumulated bacteria from within the core were being hydraulically forced through small pores that had previously been plugged off and produced as a result of the high differential pressure across the core. This phenomena caused some variations in plugging pressures, particularly toward the end of all test runs.

The data from all plugged cores were plotted showing the permeability ratio versus injected pore volumes. This information is shown on Figures 13, 14, 15, and 16, separated into core types. The best fitting smooth curve was drawn through the data points as shown. No correlation within individual rock type was apparent with respect to permeability, irreducible water saturation or pore geometry factor.

FIGURE 13

PLUGGING PLOT FOR DEVONIAN CORES

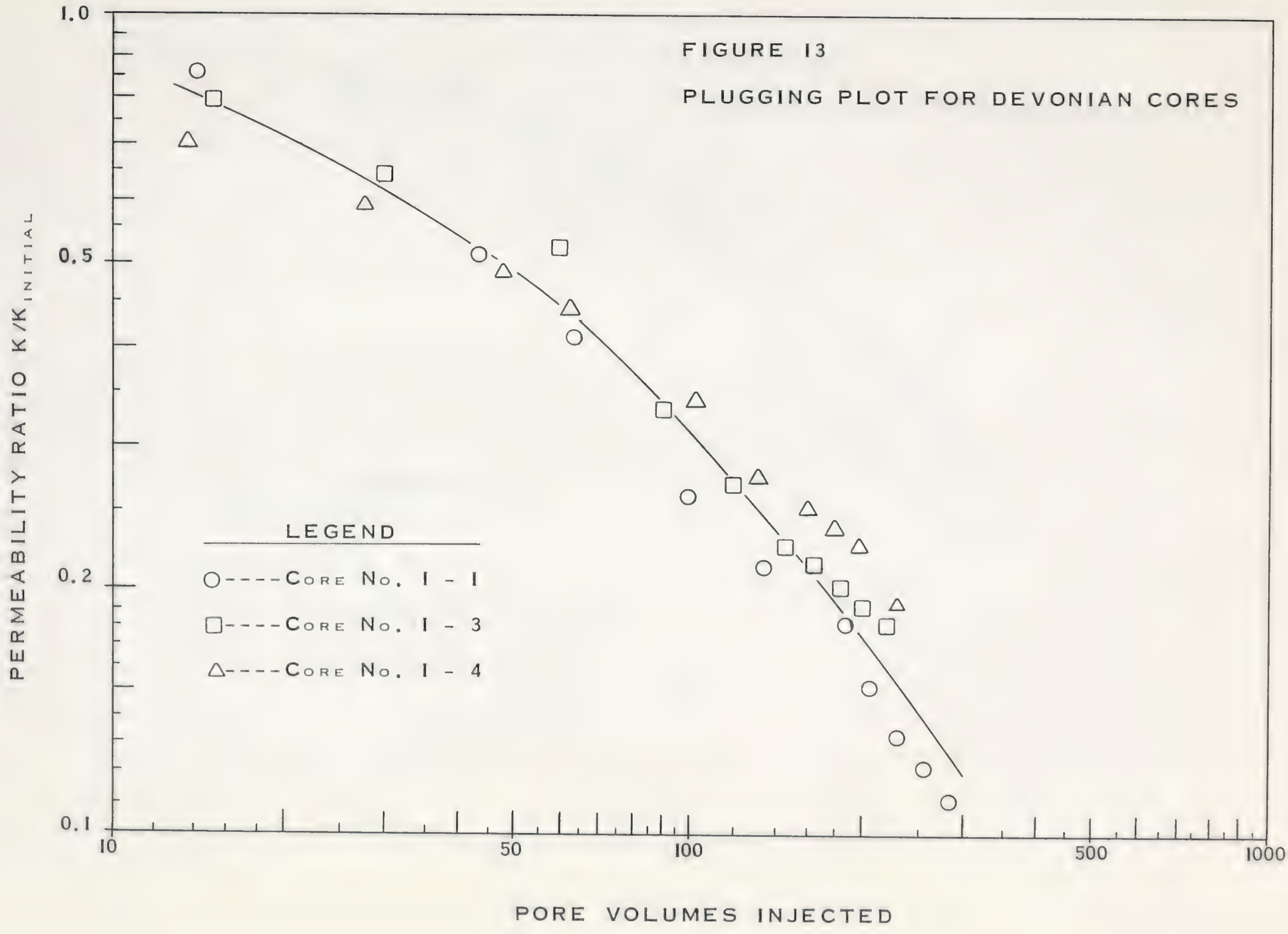

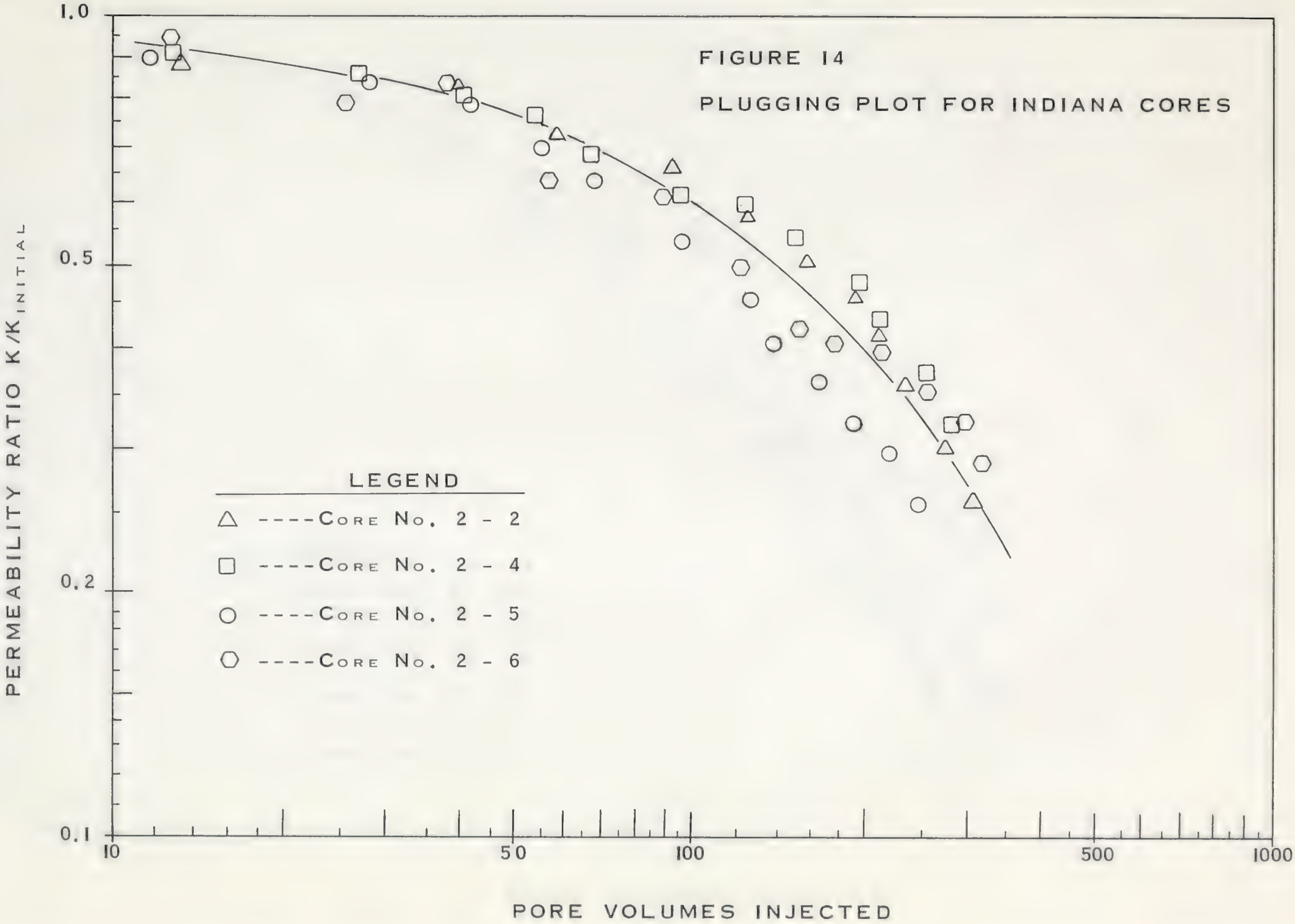

FIGURE 14

PLUGGING PLOT FOR INDIANA CORES

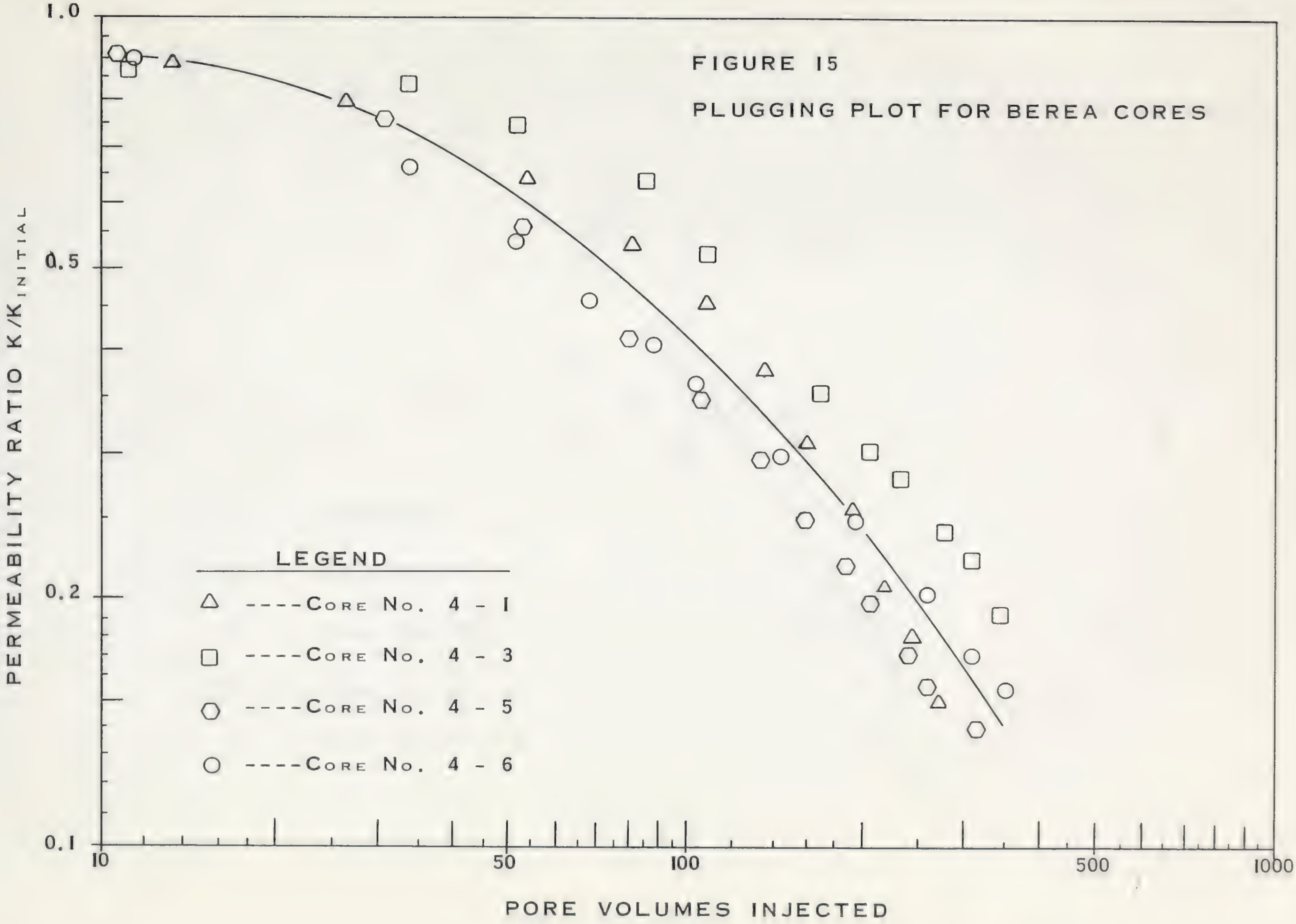

FIGURE 15

PLUGGING PLOT FOR BEREA CORES

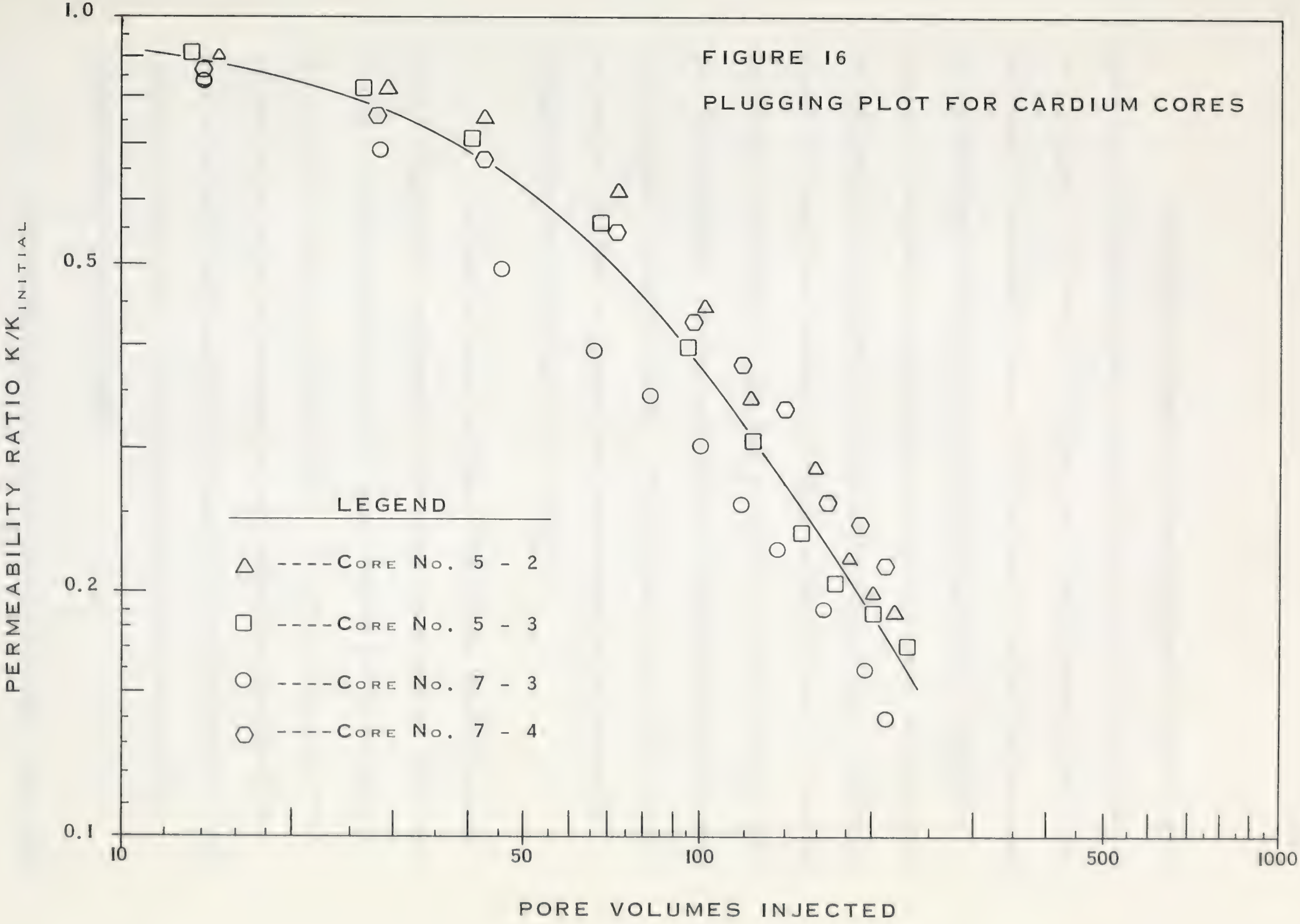

FIGURE 16

PLUGGING PLOT FOR CARDIUM CORES

The shapes of these four curves are similar, indicating the same general plugging trend. During the first portion of each injection run, plugging occurred at a relatively rapid rate as shown by the rapid decrease in permeability ratio. This was due to the fact that the small flow channel pores were easily and quickly plugged off. During the remainder of the test run the plugging rate was decreased, resulting from the additional time required for sufficient bacteria solids to accumulate within the larger pore channels to bridge and start to plug. An attempt was made to correlate average rock properties for each rock type with the rate of plugging. A summary of rock properties for the cores that were plugged is shown on Table 1. The average values of the rock properties for each type of plugged core were applied to the composite plugging plots shown on Figures 17, 18 and 19.

The results shown in Figure 17 indicated that the relative rate of plugging was independent of the initial permeability. This may be due to the fact that the property of permeability did not necessarily describe pore geometry and distribution. The rate of plugging with uniform sized solids is dependent not only on the pore geometry, but also on the distribution and rate of change of the large conductive pore channels to small pores. It was these smaller pores that could be bridged and subsequently plugged.

It was thought that irreducible water saturation values might

TABLE I

SUMMARY OF ROCK PROPERTIES

	Porosity %	Permeability md.	G-Factor	Irr. S_w%
Devonian Ls. Cores				
*1 - 1	17.8	22.0	0.5	35.5
*1 - 3	16.9	21.4	0.6	29.0
*1 - 4	18.2	49.4	0.6	32.0
1 - 6	18.0	----	1.5	28.0
Averages	17.6	30.9	0.57	32.2
Indiana Ls. Cores				
*2 - 2	19.5	5.7	0.6	----
*2 - 4	19.0	4.5	0.6	----
*2 - 5	18.5	4.8	0.7	----
*2 - 6	20.0	4.8	---	----
2 - 7	18.5	---	0.8	24.0
Averages	19.2	4.95	0.62	24.0
Berea Ss. Cores				
*4 - 1	19.0	67.2	0.3	15.8
4 - 2	19.0	----	0.3	18.4
*4 - 3	22.5	151.0	---	----
4 - 4	20.0	116.0	0.2	15.0
*4 - 5	24.0	242.0	0.2	14.5
*4 - 6	22.0	96.8	---	----
4 - 8	24.0	----	0.2	14.5
Averages	22.1	139.0	0.25	15.2
Cardium Ss. Cores				
*5 - 2	17.5	41.8	0.2	17.1
*5 - 3	18.7	44.1	---	----
5 - 4	19.0	----	0.3	18.0
*7 - 3	17.8	57.7	0.2	18.5
*7 - 4	18.0	48.5	0.2	16.7
Averages	18.0	48.2	0.2	17.4

*Plugged core properties only are used in averages.

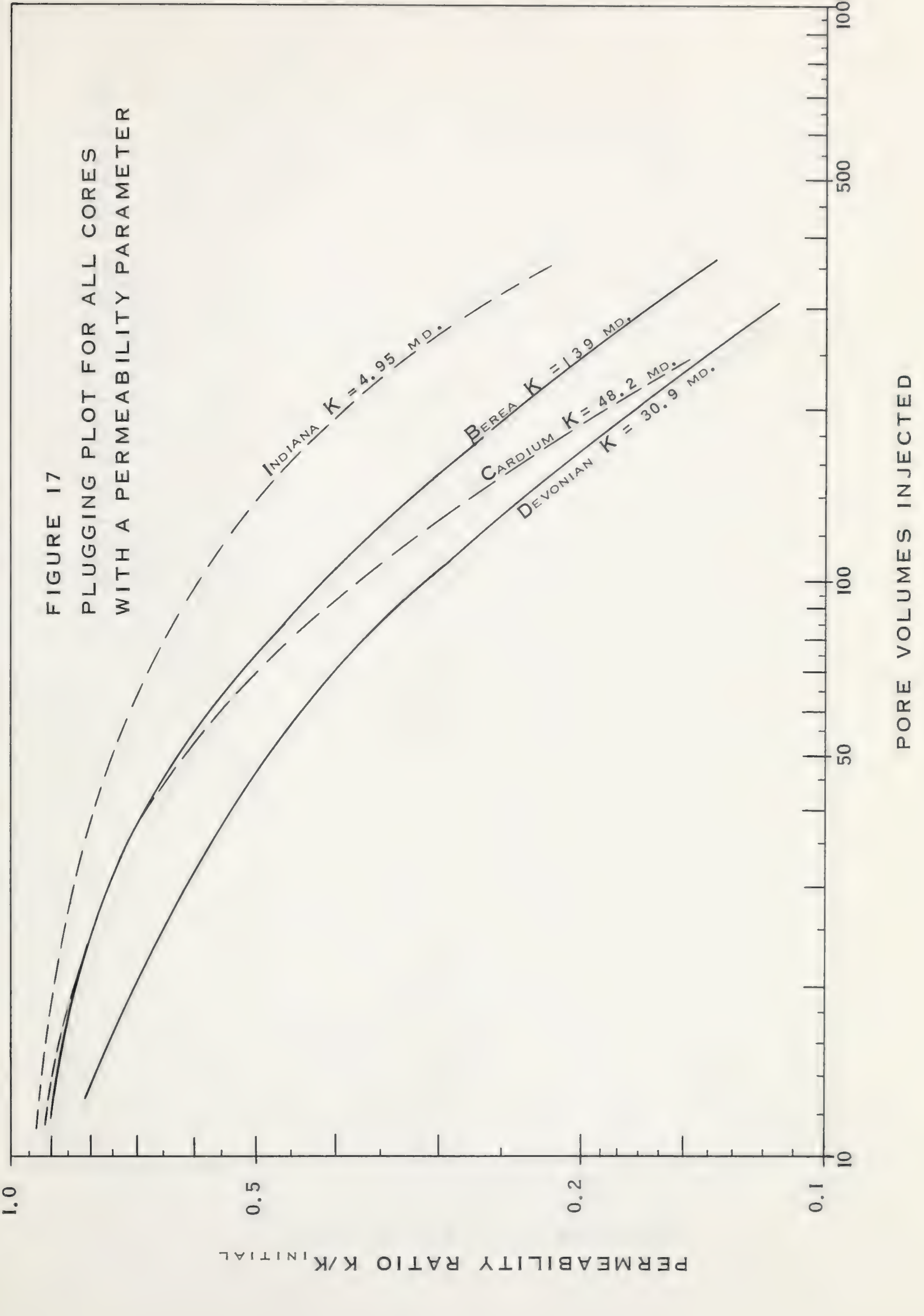

FIGURE 17

PLUGGING PLOT FOR ALL CORES WITH A PERMEABILITY PARAMETER

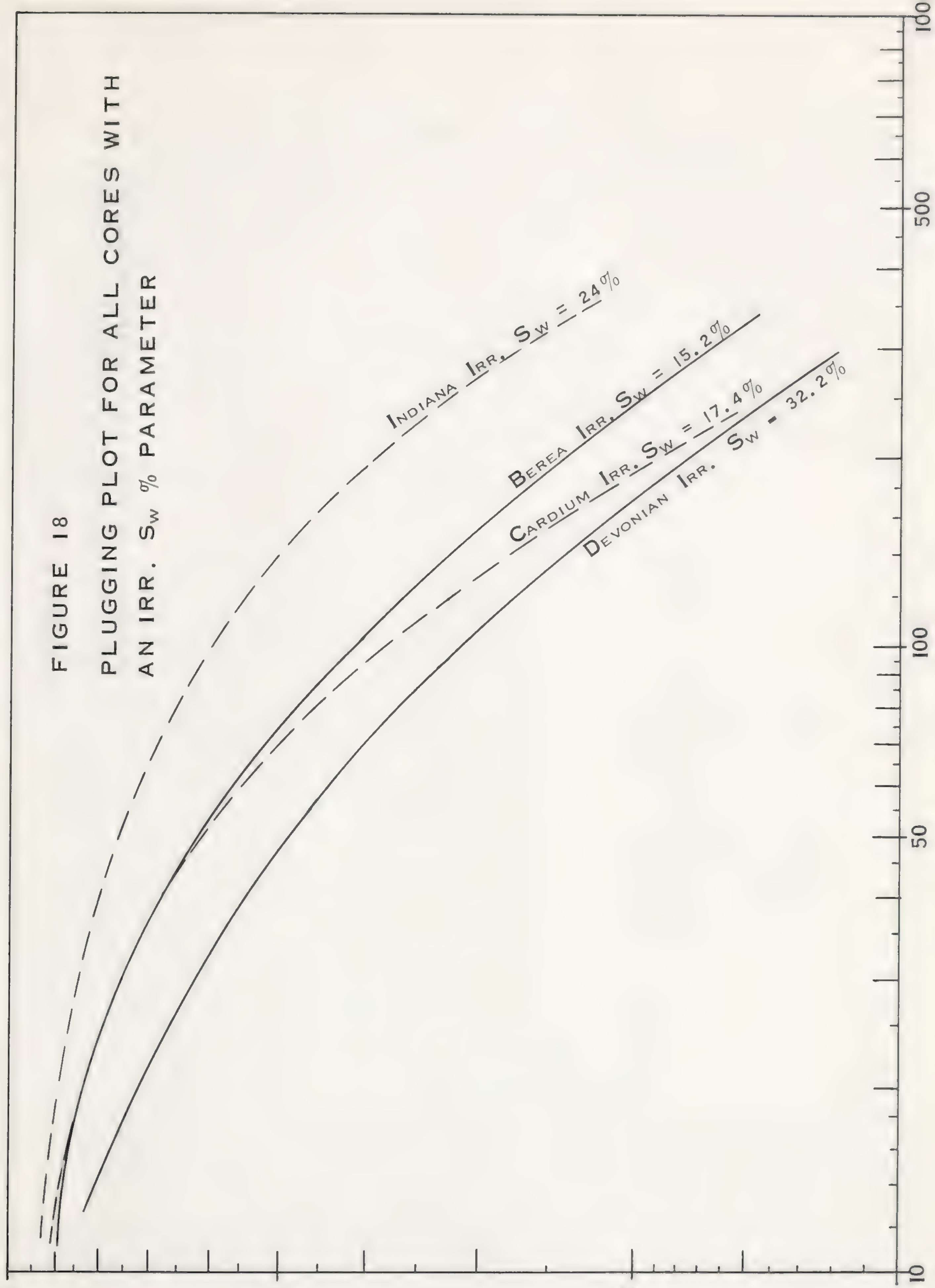

FIGURE 18

PLUGGING PLOT FOR ALL CORES WITH AN IRR. S_W % PARAMETER

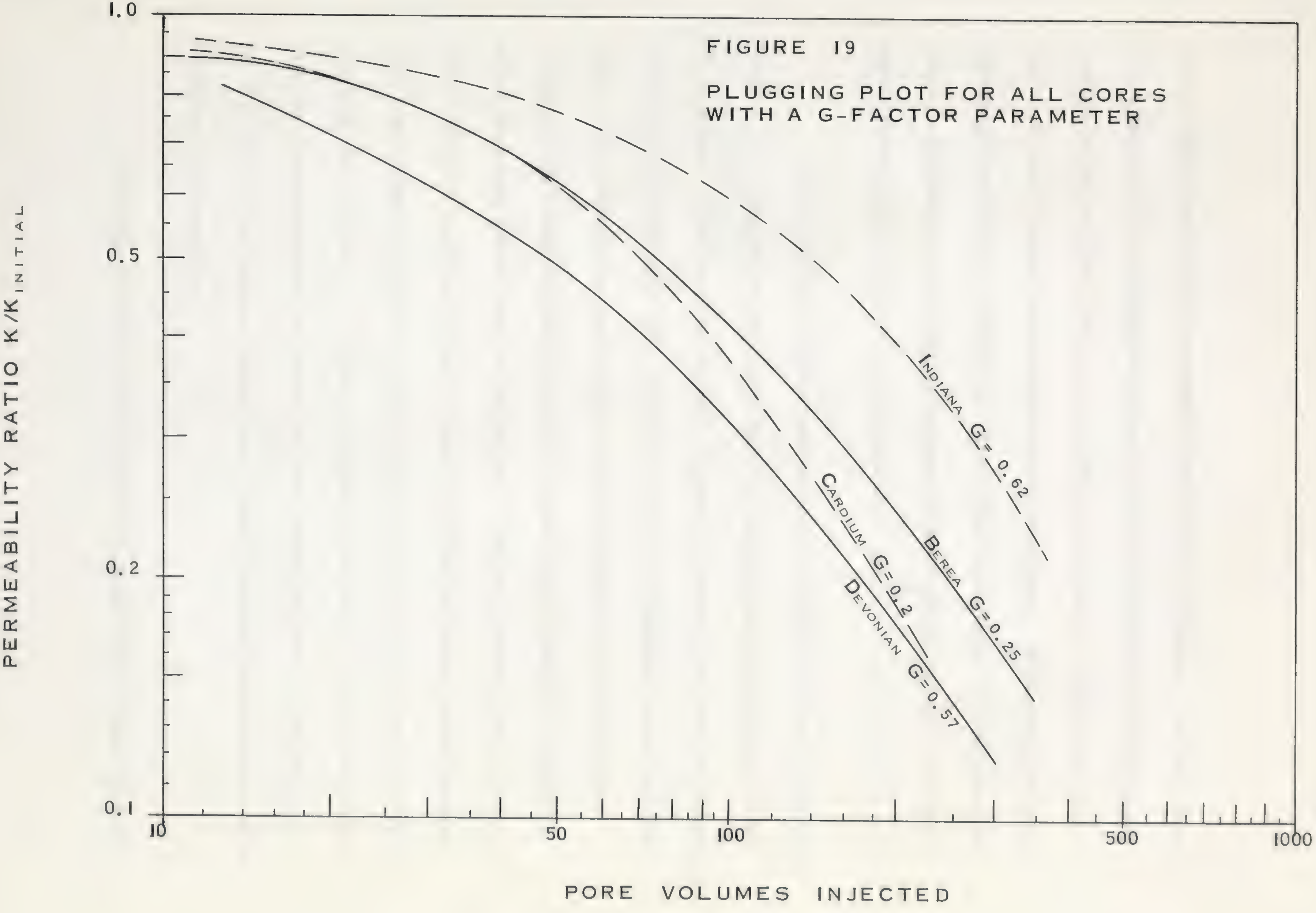

FIGURE 19

PLUGGING PLOT FOR ALL CORES
WITH A G-FACTOR PARAMETER

be a suitable correlating parameter for rate of plugging. The initiating of plugging due to bridging would occur at the entrance to a small pore system or in the finer interstices of the porous rock. These are also the locations in which irreducible water is trapped. However, the composite plot on Figure 18 does not verify this reasoning. It indicates that there is no obvious relationship between rate of plugging and irreducible water saturation in porous rock samples.

As depth of plugging was directly related to the pore geometry factor "G", it might be expected that "G" would also correlate with rate of plugging. The data contained in Figure 19 showed that rate of plugging does not correlate with "G". The curve for the Devonian cores is out of place. The reason for this could be that the distribution and rate of change of the large conductive pores to small pores was more extreme in the Devonian cores than in the others. This was evidenced by visual observation of variation in pore sizes in all the Devonian cores plugged. There were narrow regions in the cores which were the scenes of severe plugging (see Figure 11). Thus, it appears that the "G" factor indicated only the interconnection of pores and the sorting of pore sizes and does not account for the unusual variations in pore systems that occured in the Devonian core samples.

Results on Berea cores from this study were compared with

those from a previous work by Fekete(11). Generally, the plugging trends and depth of penetration were similar. However, the rate of plugging in the present study was more rapid. This was due to a number of different experimental conditions: an increase in bacteria concentration over the previous work, constant injection rate compared to an injection rate that decreased with permeability in Fekete's work and higher injection pressures that increased with plugging, compared to a constant injection pressure of 30 psig in the previous work.

Backwashing Results

Backwashing of plugged cores of all four types was carried out. Typical data was plotted on Figure 20 showing permeability ratio versus injected pore volumes. All the cores recovered 90 per cent of initial permeability by the time 600 pore volumes of brine had been injected through them.

The initial recovery of approximately one half the lost permeability was quite rapid for all cores. This could have been due to the larger and medium sized plugged pore channels recovering their conductivity more rapidly than the smaller plugged pores. Also, those plugged pores immediately adjacent to the outflow face would have started to conduct fluid almost immediately after backwashing started. The least

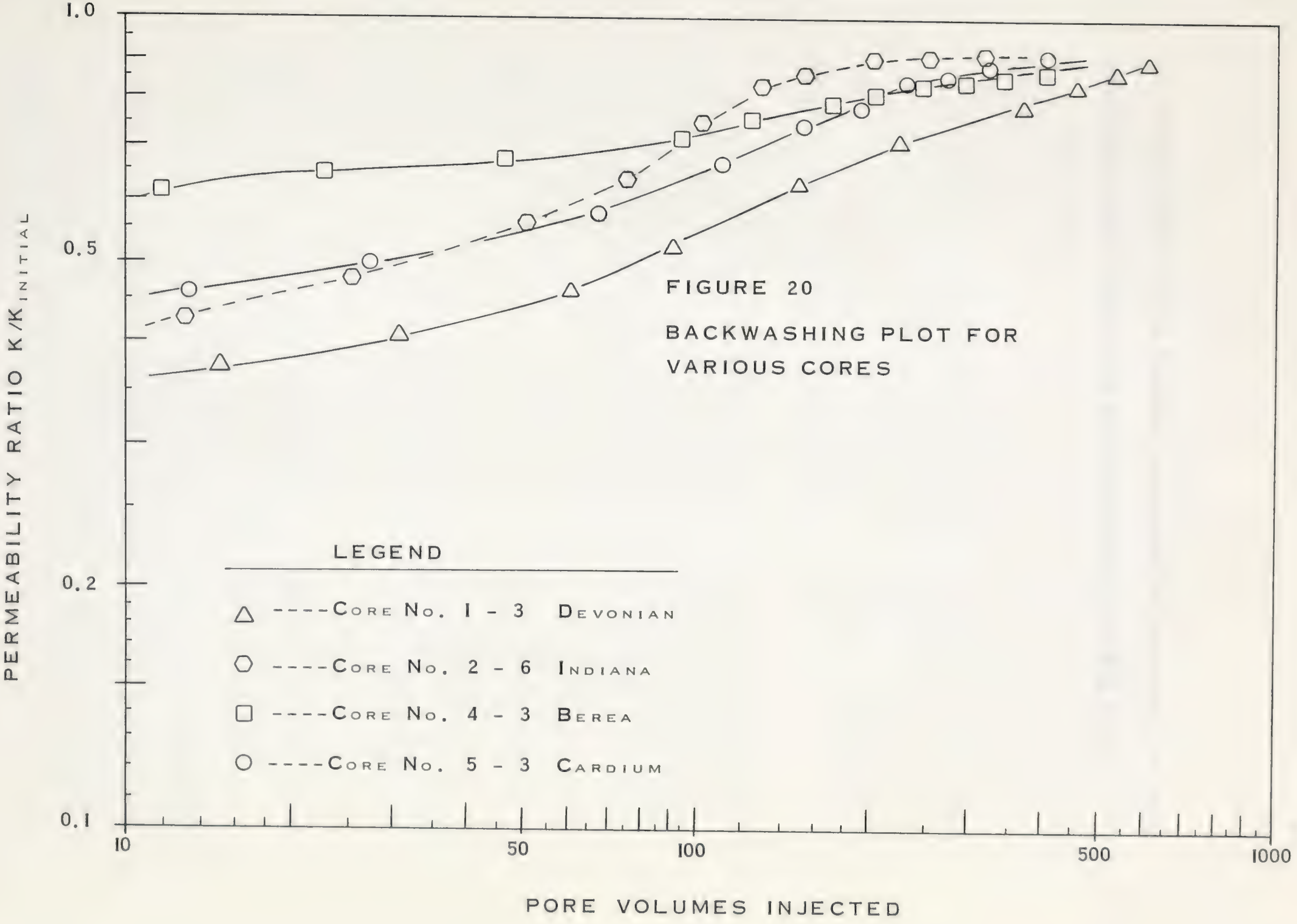

FIGURE 20

BACKWASHING PLOT FOR VARIOUS CORES

permeable Indiana cores regained permeability faster than the other three core types, even though the backwashing rate was less.

CONCLUSIONS

Reservoir rocks have extremely heterogeneous characteristics; consequently, it was difficult to justify any generalized conclusions based on their physical properties with regard to plugging behavior. However, the following qualitative statements are of interest with regard to physical rock properties and the process of injection plugging in reservoirs. They are necessarily restricted to the four rock types studied and the limited laboratory tests performed.

1) Desaturation capillary pressure curves indicated that the two types of carbonate cores studied have multi-pore systems believed to be due to a combination of primary and secondary porosity effects. This was verified by the general curve shape similarities of mercury injection capillary pressure curves and by visual inspection.

2) Wettability imbibition tests indicated that the Devonian and Cardium cores were less water-wet than the Indiana and Berea cores. This relative wettability difference affected the shape and location of capillary pressure curves and dependent properties. To nullify wettability effects, some increase in the values shown for pore geometry factor "G" and irreducible water saturation would be required for the Devonian and Cardium cores. The exact amount of this increase was not known because the contact angles could not be measured. Nevertheless, the following points are still valid.

3) Depth of plugging was a function of the pore geometry factor "G". In rocks with homogeneous pore sizes, pore bridging was initiated by bacteria almost immediately upon entering the core body. Consequently, the majority of plugging was confined to a narrow cylinder of core adjacent to the inlet face. In the heterogeneous cores, some minor amounts of plugging occurred at the inlet face possibly due to small pore sizes plugging off. However, most of the bacteria solids were carried within the larger pore channels into the core body where the majority of plugging occurred.

4) Rate of plugging with uniform sized solids was dependent not only on the pore geometry, but also on the distribution and rate of change of the large pore channels to small pores. It was these smaller pores that could be bridged and subsequently plugged. The pore geometry factor "G" did not seem to indicate the distribution and rate of change of the large to small conductive pore sizes and thus did not correlate to rate of plugging.

5) The pore geometry factor "G" was a measure of the sorting and interconnection of the various pore sizes. It was the significant petrophysical rock characteristic for depth of plugging but failed as a parameter for rate of plugging. The "G" factor does not seem to completely describe porous rock geometry for plugging predictions.

6) Neither permeability nor irreducible water saturation correlated with rate of plugging. These two physical rock properties did not appear to directly reflect the two parameters for rate of plugging.

7) No known measurable physical rock property would account for the unusual pore systems that occurred in the Devonian limestone core samples. The abrupt variation in pore sizes was the scene of very severe plugging.

8) The general plugging trend was the same for all core types. During the first portion of each injection run, plugging occurred at a relatively rapid rate. This was due to the fact that the small flow channel pores were quickly plugged off. During the remainder of the test run the plugging rate was decreased, resulting from the additional time required for sufficient bacteria to accumulate within the larger pore channels, to bridge and start to plug.

9) Toward the end of the test runs it appeared, periodically, that some accumulated bacteria from within the core were being hydraulically forced through small pores which had previously been plugged off. This accumulated bacteria then plugged downstream pores or was produced with the effluent. This phenomena was caused by high differential pressure across the core and caused fluctuating pressure readings.

10) Backwashing results indicated that all plugged core types recovered 90 per cent of initial permeability by the time 600 pore volumes of brine had been injected through them. The initial recovery of approximately one half the lost permeability was quite rapid for all cores. This was attributed to the larger and medium sized pore channels recovering their conductivity more rapidly than the smaller plugged pores.

RECOMMENDATIONS

This work has attempted to relate rock properties to plugging trends. Four types of rock and one type of bacteria were studied. Although the results of this work were not completely successful, they are sufficiently encouraging to warrant further investigations into this problem.

Two great unsolved problems in petroleum research caused difficulties in this study. They were lack of a quantitative measure of wettability and a single factor to completely describe the geometrical property of porous media. Future studies should use porous material chemically treated to make them fully water-wet and fairly uniform porous rock, such as Berea sandstone, whose pore system might be adequately described by the pore geometry factor "G" or another suitable factor.

The laboratory affect of injection rate and pressure on plugging has not been investigated and would make a worthwhile contribution to knowledge of the nature of plugging in porous media. In order to remove as many other variables as possible, this research work might be conducted using a uniform-grained, fully water-wet, unconsolidated sand system, with a constant bacteria solids concentration.

The effect of bacteria solids for plugging, used in laboratory

work, should be investigated using a greater variety of concentration, more in line with field injection system concentrations. Then, plugging results obtained, in the laboratory, with a high count of solids and field cores may be related directly to field operations. Only one bacteria type, Bacillus subtilis, has been used for plugging. The effect on porous rocks of other bacteria commonly found in injection water, and that can be easily cultured, would be of interest.

NOMENCLATURE

A - Cross-sectional area in square centimetres.

API - American Petroleum Institute.

atm. - Atmospheres.

cc - Cubic centimetres.

cms - Centimetres.

cms Hg - Pressure in centimetres of mercury.

D. P. - Displacement pressure.

e - Naperian Constant = 2.71828····

G - Pore Geometry Factor.

Hg curve - Mercury injection capillary pressure curve.

Irr S_w - Irreducible water saturation.

K - Permeability in darcys or millidarcys.

K_i - Initial permeability of the core.

L - Length in centimetres.

Ls - Limestone.

md - Millidarcy = 0.001 darcys.

mins - Minutes.

P_c - Capillary pressure.

P_d - Displacement pressure.

P_{nw} - Pressure in the non-wetting phase.

Psi - Pounds per square inch.

Psia - Pounds per square inch absolute.

Psig - Pounds per square inch gauge pressure.

NOMENCLATURE (CONTINUED)

P. V. - Pore volumes injected.

P_w - Pressure in the wetting phase or pressure in the water phase.

$\triangle P$ - Pressure differential in atmospheres or pounds per square inch.

Q - Flow rate in cubic centimetres per second.

r - Radius of a capillary.

sec - Second.

S_{nw} - Saturation of the non-wetting phase.

Ss - Sandstone.

S_w - Saturation of the wetting phase or water saturation.

$(V_b)_{P_c}$ - Fractional bulk volume occupied by the displacing fluid at any capillary pressure.

$(V_b)_{P_\infty}$ - Fractional bulk volume occupied by the displacing fluid at infinite pressure or total interconnected pore volumes.

Vol. - Volume.

Vols. - Volumes.

σ - Interfacial tension.

θ - Contact angle.

μ - Viscosity in centipoises.

% - Per cent.

BIBLIOGRAPHY

1. Amyx, J.W., Bass, D.M., and Whiting, R.L.: "Petroleum Reservoir Engineering - Physical Properties", Chapter 2, McGraw-Hill Book Company Inc., (1960).

2. Beck, J.V.: "The Role of Bacteria in Oil Production", Prod. Monthly (July 1946), p29.

3. Beck, J.V.: "Prevention of Microbiological Growths in Water Flood Operations", Prod. Monthly (October 1947), p21.

4. Bobek, J.E., Mattax, C.C. and Denekas, M.O.: "Reservoir Rock Wettability - Its Significance and Evaluation", Trans AIME (1958), Vol. 213, p155.

5. Buck, J. Randolph: "Elements of Water Injection", The Petroleum Engineer, Reader Services Reprint.

6. Burdine, N.T., Gournay, L.S. and Reicherty, P.O.: "Pore Size Distribution of Reservoir Rocks", Trans. AIME (1950), Vol. 189, p195.

7. Calhoun, John C. Jr.: "Fundamentals of Reservoir Engineering", Part II, University of Oklahoma Press, (1953).

8. Carlson, V., Bennett, E.O. and Rowe, J.A.: "The Variety and Recurrence of Microbial Flora and Their Relation to Water Quality in a Number of Oilfield Water Injection Systems", Preprint AIME Annual Fall Meeting (1960).

9. Collins, R.E.: "Flow of Fluids Through Porous Materials", Chapters 1 and 2, Reinhold Publishing Corp. (1961).

10. Crawford, P.B.: "Continual Changes Observed in Bacterial Stratification Rectification", Prod. Monthly, (February 1962), p12.

11. Fekete, T.: "The Plugging Effect of Bacteria in Sandstone Systems", M.Sc. Thesis, Unpublished, University of Alberta (1959).

12. Gatlin, Carl: "Petroleum Engineering: Drilling and Well Completions", Chapters 10 and 12, Prentice-Hall Inc. (1960).

13. Gatlin, Carl and Nemir, C. E.: "Some Effects of Size Distribution on Particle Bridging in Lost Circulation and Filtration Tests", J.P.T., (June 1961), p575.

14. Glen, E.E. and Slusser, M.L.: "Drilling Fluid Particle Invasion into Porous Media", J.P.T., (May 1957), p132.

15. Hart, R.T., Fekete, T. and Flock, D.L.: "The Plugging Effect of Bacteria in Sandstone Systems", Oil in Canada, (April 6, 1961), p60.

16. Katz, D.L., Turner, C.E., Grimm, R.D., Elenbaas, J.R. and Vary, J.A.: "Sample Grading Method of Estimating Gas Reserves", Trans. AIME (1952), Vol. 195, p207.

17. Krueger, R.F. and Vogel, L.C.: "Damage to Sandstone Cores by Particles from Drilling Muds", API Drilling and Production Practices, (1954), p158.

18. McKetta, J.J., Wehe, A.H.: "Petroleum Production Handbook", Chapter 22, McGraw-Hill Book Company Inc., (1962).

19. Merkt, E.E.: "The Effect of Bacteria on the Permeability of Oil Reservoir Rock", M.Sc. Thesis, Unpublished, University of Texas, (1943).

20. Myers, G.E. and Slabyj, B.M.: "The Microbiological Quality of Injection Water Used in Alberta Oil-Fields", Prod. Monthly, (May 1962), p12.

21. Nowak, T.J. and Krueger, R.F.: "The Effect of Mud Filtrate and Mud Particles upon the Permeability of Cores", API Drilling and Production Practices (1951), p164.

22. Perry, John H.: "Chemical Engineers' Handbook", Third Ed. p374, McGraw-Hill Book Company Inc., (1950).

23. Pirson, S.J.: "Oil Reservoir Engineering", Chapters 1,2, and 7, 2nd Ed., McGraw-Hill Book Company Inc., (1958).

24. Purcell, W.R.: "Capillary Pressures - Their Measurement Using Mercury and the Calculation of Permeability Therefrom, Trans. AIME (1949), Vol. 186, p111.

25. "Recommended Practices for Determining Permeability of Porous Media", American Petroleum Institute, API Code 27, Division of Production (1952).

26. Rose, W. and Bruce, W.A.: "Evaluation of Capillary Character in Petroleum Reservoir Rock", Trans AIME (1949), Vol. 186, p127.

27. Scheidegger, A.E.: "The Physics of Flow Through Porous Media", Parts 1, 2 and 3, Rev. Ed., University of Toronto Press (1960).

28. Thomeer, J.H.M.: "Introduction of a Pore Geometrical Factor Defined by the Capillary Pressure Curve", Trans AIME (1960), Vol. 219, p354.

29. Thornton, O.F. and Marshall, D.L.: "Estimating Interstitial Water by the Capillary Method", Trans AIME (1947), Vol. 170, p69.

30. Uren, L.C.: "Petroleum Production Engineering: Oilfield Exploitation", Chapter 1, 3rd Ed., McGraw-Hill Book Company Inc. (1953).

31. Whiting, R.L. and Guerrero, E.T.: "Capillary Properties of Some Limestone Cores", Oil and Gas Journal, July 26, 1951, p272.

32. Wright, C.C.: "What We're Learning About Bacterial Corrosion", Oil and Gas Journal, June 25, 1962, p124.

APPENDIX

TABLE 2

CAPILLARY PRESSURE CURVE DATA FOR CORE NO. 1 - 1

Devonian Ls.

Bulk Volume = 41.15 cc
Pore Volume = 7.33 cc

P_c Cms. Hg.	Cumulative Displaced Vol. cc	S_{nw} as Fraction of Bulk Vol.	% S_w	Days to Equilibrium
2.5	0.45	0.011	93.9	4
5.0	1.07	0.026	85.4	3
7.5	1.48	0.036	79.8	3
10.0	1.57	0.038	78.6	3
15.0	1.73	0.042	76.4	3
20.0	1.85	0.045	74.7	3
25.0	2.14	0.052	70.8	3
30.0	2.67	0.065	63.5	3
40.0	3.33	0.081	54.6	3
50.0	3.70	0.090	49.5	3
60.0	3.98	0.097	45.7	3
80.0	4.31	0.105	41.2	4
100.0	4.40	0.107	40.0	4
∞	---	0.115	35.5	---

TABLE 3

CAPILLARY PRESSURE CURVE DATA FOR CORE NO. 1 - 3

Devonian Ls.

Bulk Volume = 40.71 cc
Pore Volume = 6.88 cc

Pc Cms. Hg.	Cumulative Displaced Vol. cc	S_{nw} as Fraction of Bulk Vol.	% S_w	Days to Equilibrium
2.5	0.0	0.0	100.0	4
5.0	0.53	0.013	92.2	3
7.5	0.77	0.019	88.8	3
10.0	0.98	0.024	85.7	3
15.0	1.34	0.033	80.5	3
20.0	1.87	0.046	72.8	3
25.0	2.32	0.057	66.3	3
30.0	2.52	0.062	63.4	3
40.0	2.81	0.069	59.2	3
50.0	3.18	0.078	53.7	3
60.0	3.66	0.090	46.8	3
80.0	4.07	0.100	40.9	4
100.0	4.60	0.113	33.2	4
∞	---	0.120	29.0	---

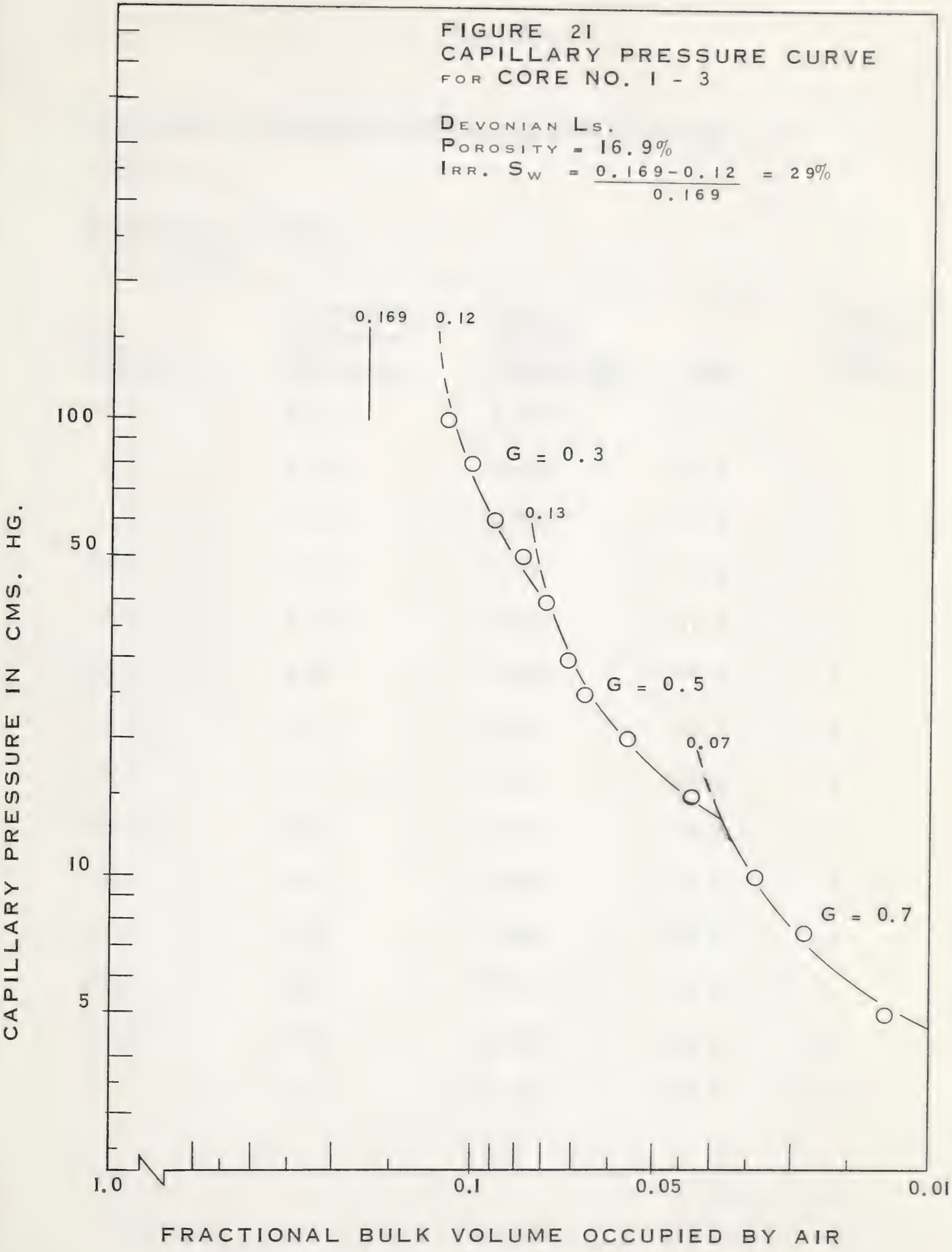

FIGURE 21
CAPILLARY PRESSURE CURVE
FOR CORE NO. 1 - 3

Devonian Ls.
Porosity = 16.9%
Irr. $S_w = \frac{0.169-0.12}{0.169} = 29\%$

TABLE 4

CAPILLARY PRESSURE CURVE DATA FOR CORE NO. 1 - 4

Devonian Ls.

Bulk Volume = 40.65 cc
Pore Volume = 7.40 cc

Pc Cms. Hg.	Cumulative Displaced Vol. cc	S_{nw} as Fraction of Bulk Vol.	% S_w	Days to Equilibrium
2.5	0.49	0.012	93.4	4
5.0	1.14	0.028	84.6	3
7.5	1.43	0.035	80.7	3
10.0	1.71	0.042	76.9	3
15.0	2.12	0.052	71.3	3
20.0	2.40	0.059	67.5	3
25.0	2.73	0.067	63.1	3
30.0	2.89	0.071	60.9	3
40.0	3.05	0.075	58.8	3
50.0	3.26	0.080	55.9	3
60.0	3.54	0.087	52.2	3
80.0	4.26	0.105	42.3	4
100.0	4.76	0.117	35.6	4
∞	---	0.125	32.0	---

TABLE 5

CAPILLARY PRESSURE CURVE DATA FOR CORE NO. 1 - 6 USING MERCURY

Porosity = 18.0%

Bulk Volume of Plug = 28.76 - (22.16 - 12.03) = 18.63 cc

*Corrected Pressure P_c Psia	Hg. Fraction of Bulk Volume
1.8	(12.03 - 11.82) / 18.63 = 0.011
3.0	(12.03 - 11.70) / 18.63 = 0.018
4.6	(12.03 - 11.62) / 18.63 = 0.022
8.2	(12.03 - 11.49) / 18.63 = 0.029
13.1	(12.03 - 11.11) / 18.63 = 0.042
18.3	(12.03 - 11.02) / 18.63 = 0.054
26.5	(12.03 - 10.85) / 18.63 = 0.063
36.8	(12.03 - 10.67) / 18.63 = 0.073
48.0	(12.03 - 10.56) / 18.63 = 0.079
65.0	(12.03 - 10.45) / 18.63 = 0.085
84.0	(12.03 - 10.39) / 18.63 = 0.088
111.0	(12.03 - 10.28) / 18.63 = 0.094
214.0	(12.03 - 10.07) / 18.63 = 0.105
352.0	(12.03 - 10.04) / 18.63 = 0.107
518.0	(12.03 - 9.98) / 18.63 = 0.112

*Includes 1.5 psia to account for height of mercury above core plug.

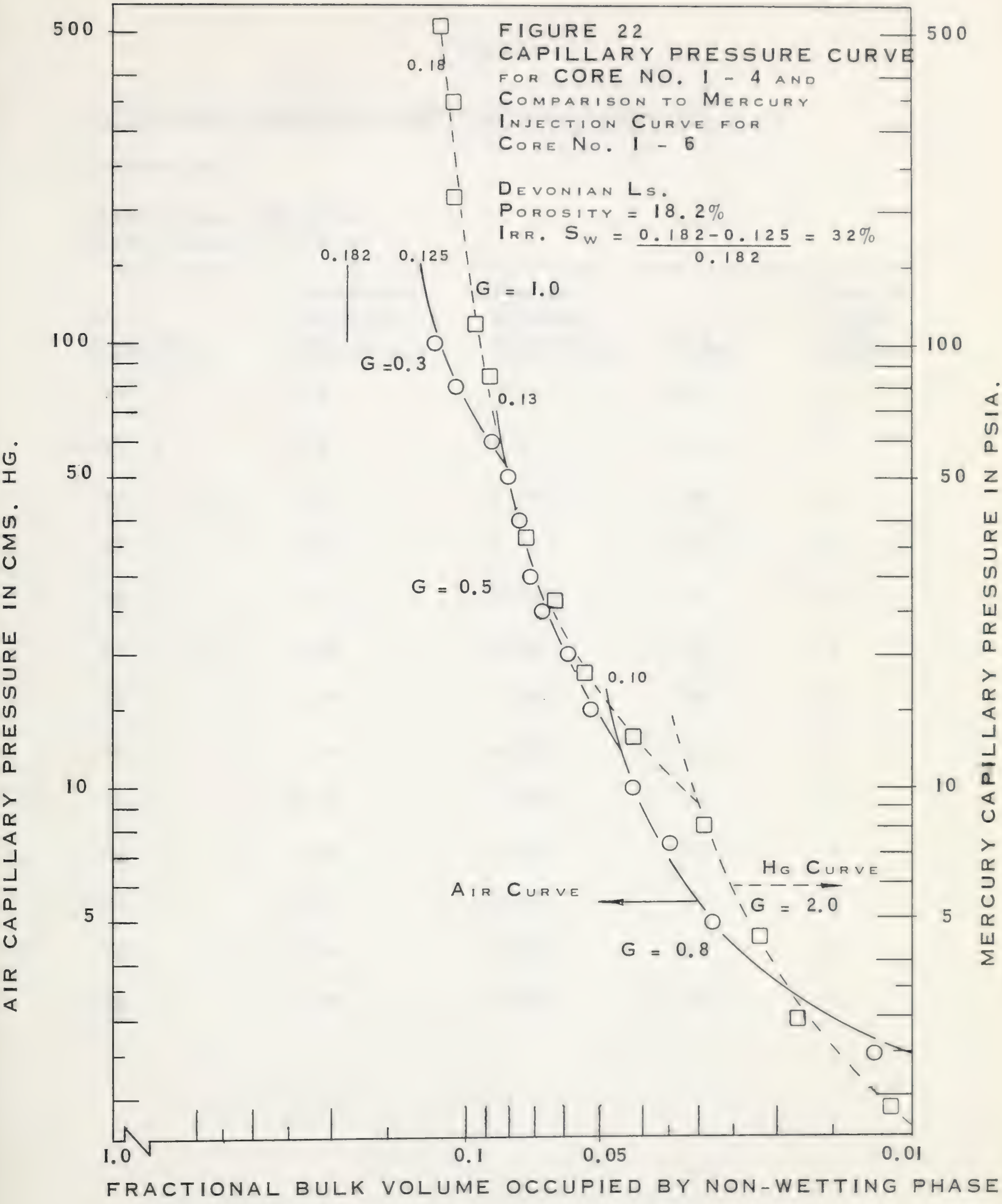

FIGURE 22
CAPILLARY PRESSURE CURVE
FOR CORE NO. I - 4 AND
COMPARISON TO MERCURY
INJECTION CURVE FOR
CORE NO. I - 6

DEVONIAN LS.
POROSITY = 18.2%
IRR. $S_W = \frac{0.182-0.125}{0.182} = 32\%$

TABLE 6

CAPILLARY PRESSURE CURVE DATA FOR CORE NO. 2 - 2

Indiana Ls.

Bulk Volume = 40.25 cc
Pore Volume = 7.85 cc

P_c Cms. Hg	Cumulative Displaced Vol. cc	S_{nw} as Fraction of Bulk Vol.	% S_w	Days to Equilibrium
30	0.0	0.0	100	3
40	0.0	0.0	100	3
45	0.47	0.011	94	4
50	0.55	0.013	93	3
55	0.71	0.017	91	3
60	0.86	0.021	89	3
65	0.94	0.023	88	3
70	1.18	0.029	85	3
75	2.04	0.050	74	4
80	2.52	0.062	68	3
85	2.67	0.066	66	3
90	2.83	0.070	64	3
100	2.98	0.073	62	4

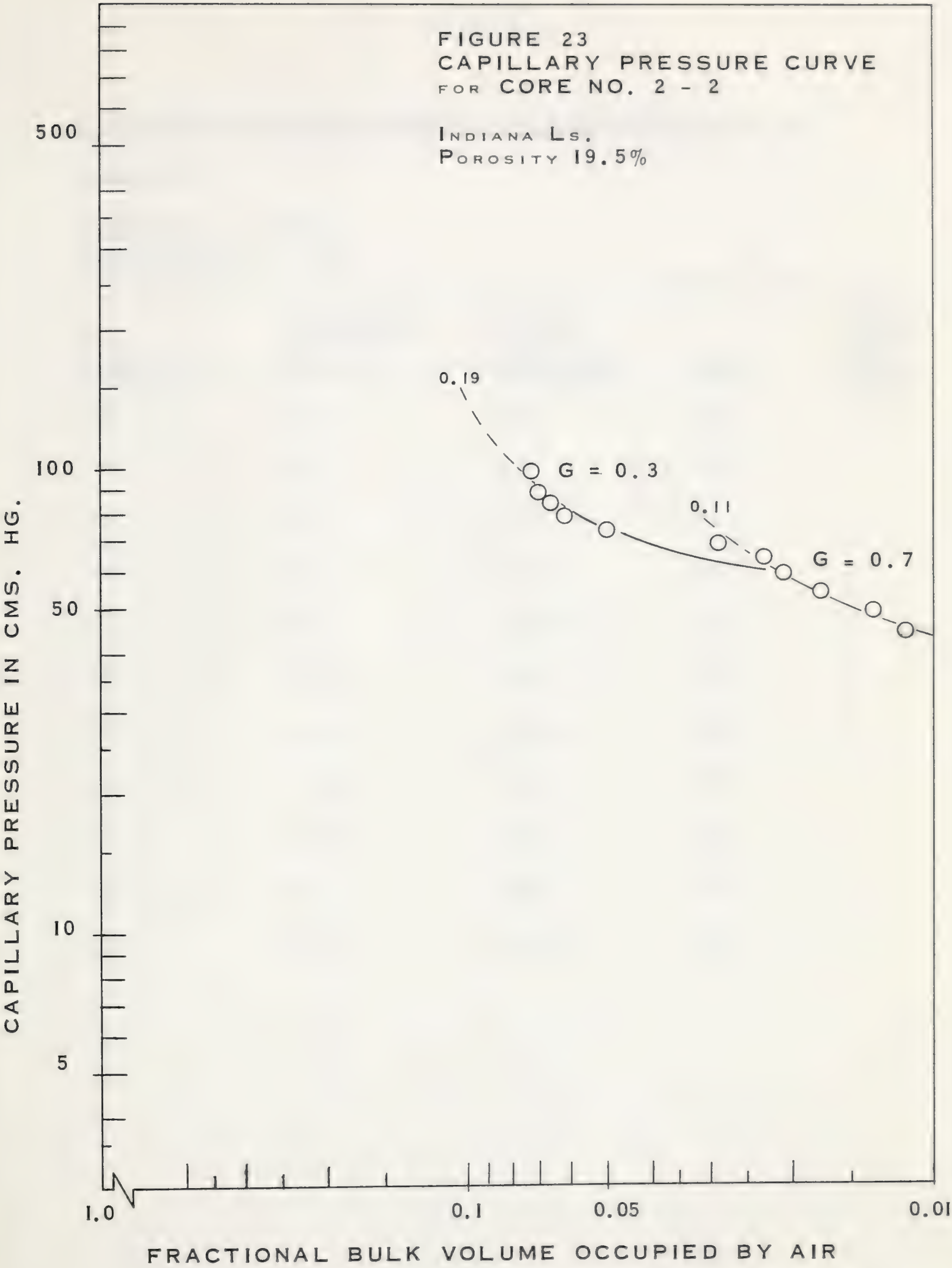

FIGURE 23
CAPILLARY PRESSURE CURVE
FOR CORE NO. 2 - 2
INDIANA LS.
POROSITY 19.5%
0.19
G = 0.3
0.11
G = 0.7
500
100
50
10
5
CAPILLARY PRESSURE IN CMS. HG.
1.0
0.1
0.05
0.01
FRACTIONAL BULK VOLUME OCCUPIED BY AIR

TABLE 7

CAPILLARY PRESSURE CURVE DATA FOR CORE NO. 2 - 4

Indiana Ls.

Bulk Volume = 40.55 cc
Pore Volume = 7.71 cc

P_c Cms. Hg.	Cumulative Displaced Vol. cc	S_{nw} as Fraction of Bulk Vol.	% S_w	Days to Equilibrium
40	0.0	0.0	100	3
50	0.0	0.0	100	3
55	0.49	0.012	94	3
60	0.65	0.016	92	3
65	0.77	0.019	90	3
70	0.93	0.023	88	3
75	1.21	0.030	84	4
80	1.54	0.038	80	3
85	1.98	0.049	74	3
90	2.31	0.057	70	3
100	2.60	0.064	66	4

TABLE 8

CAPILLARY PRESSURE CURVE DATA FOR CORE NO. 2 - 5

Indiana Ls.

Bulk Volume - 40.25 cc
Pore Volume - 7.45 cc

P_c Cms. Hg.	Cumulative Displaced Vol. cc	S_{nw} as Fraction of Bulk Vol.	% S_w	Days to Equilibrium
30	0.0	0.0	100	3
35	0.48	0.012	94	3
40	0.60	0.015	92	3
45	0.68	0.017	91	3
50	0.84	0.021	89	3
55	1.09	0.027	85	3
60	1.37	0.034	82	3
65	1.61	0.040	78	3
70	1.77	0.043	76	3
75	1.89	0.047	75	4
80	2.05	0.051	72	3
85	2.22	0.055	70	3
90	2.50	0.062	66	3
100	2.74	0.068	63	4

TABLE 9

CAPILLARY PRESSURE CURVE DATA FOR CORE NO. 2 - 7 USING MERCURY

Porosity = 18.5%

Bulk Volume of Plug = 28.76 - (15.90 - 4.97) = 17.83 cc

*Corrected Pressure P_c Psia	Hg. Fraction of Bulk Volume
26	(4.97 - 4.77) / 17.83 = 0.011
40	(4.97 - 4.72) / 17.83 = 0.014
57	(4.97 - 4.61) / 17.83 = 0.020
68	(4.97 - 4.38) / 17.83 = 0.033
87	(4.97 - 4.13) / 17.83 = 0.047
105	(4.97 - 4.01) / 17.83 = 0.054
155	(4.97 - 3.60) / 17.83 = 0.077
245	(4.97 - 2.97) / 17.83 = 0.112
360	(4.97 - 2.69) / 17.83 = 0.128
500	(4.97 - 2.51) / 17.83 = 0.137

*Includes 1.5 psia to account for height of mercury above core plug.

TABLE 10

CAPILLARY PRESSURE CURVE DATA FOR CORE NO. 4 - 1

Berea Ss.

Bulk Volume = 40.40 cc
Pore Volume = 7.73 cc

P_c Cms. Hg.	Cumulative Displaced Vol. cc	S_{nw} as Fraction of Bulk Vol.	% S_w	Days to Equilibrium
5	0.0	0.0	100	3
8	1.39	0.035	82.0	2
10	2.88	0.071	62.8	2
15	3.78	0.094	51.0	2
20	4.32	0.107	44.0	2
30	4.83	0.120	37.5	2
40	5.05	0.125	34.6	2
50	5.35	0.133	30.8	2
60	5.60	0.139	27.5	2
80	5.86	0.145	24.0	3
100	6.10	0.151	21.0	3
∞	---	0.160	15.8	---

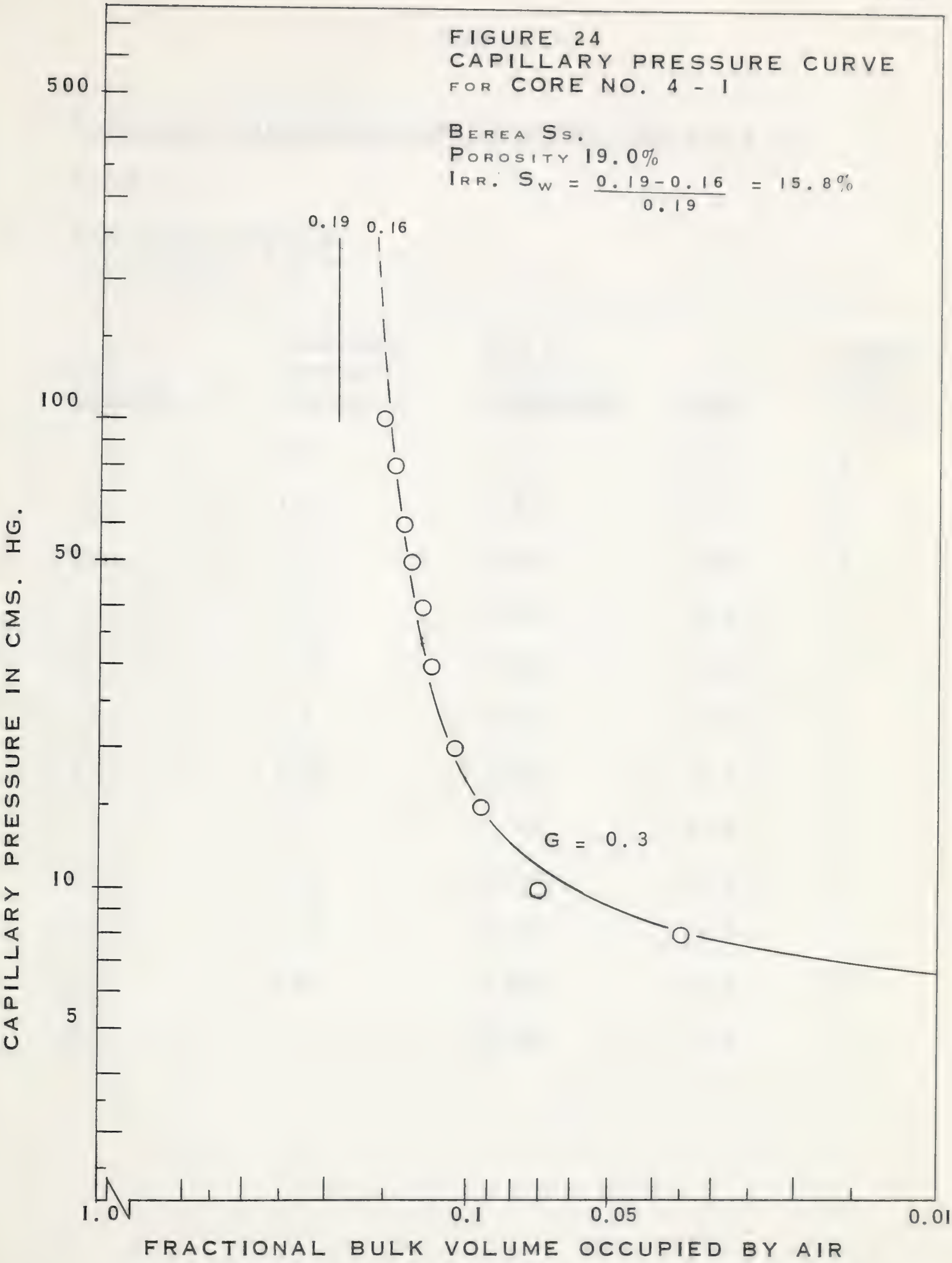

FIGURE 24
CAPILLARY PRESSURE CURVE
FOR CORE NO. 4 - 1

BEREA SS.
POROSITY 19.0%
IRR. $S_W = \frac{0.19-0.16}{0.19} = 15.8\%$

TABLE 11

CAPILLARY PRESSURE CURVE DATA FOR CORE NO. 4 - 2

Berea Ss.

Bulk Volume = 40.50 cc
Pore Volume = 7.67 cc

P_c Cms. Hg.	Cumulative Displaced Vol. cc	S_{nw} as Fraction of Bulk Vol.	% S_w	Days to Equilibrium
5	0.0	0.0	100	3
8	1.47	0.034	81.8	2
10	2.72	0.067	64.6	2
15	3.70	0.091	51.8	2
20	4.33	0.107	43.5	2
30	4.81	0.118	37.3	2
40	5.06	0.125	34.0	2
50	5.36	0.132	30.0	2
60	5.56	0.137	27.5	2
80	5.78	0.143	24.5	3
100	6.02	0.148	21.5	3
∞	---	0.155	18.4	---

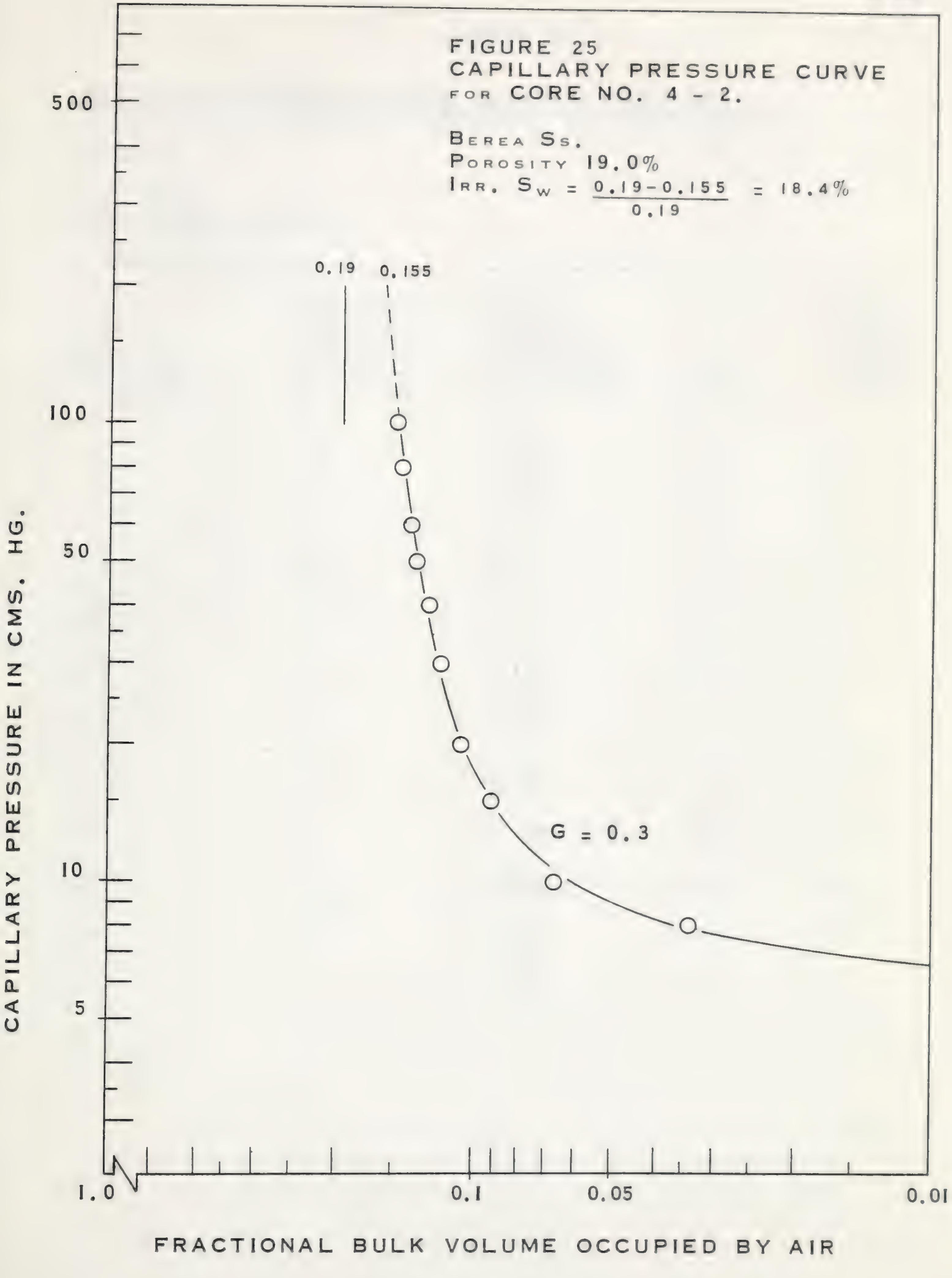

FIGURE 25
CAPILLARY PRESSURE CURVE
FOR CORE NO. 4 - 2.

Berea Ss.
Porosity 19.0%
Irr. $S_W = \frac{0.19-0.155}{0.19} = 18.4\%$

TABLE 12

CAPILLARY PRESSURE CURVE DATA FOR CORE NO. 4 - 4

Berea Ss.

Bulk Volume = 42.25 cc
Pore Volume = 8.45 cc

P_c Cms. Hg.	Cumulative Displaced Vol. cc	S_{nw} as Fraction of Bulk Vol.	% S_w	Days to Equilibrium
5	0.0	0.0	100	3
8	1.54	0.037	81.8	2
10	3.10	0.074	63.3	2
15	4.96	0.118	41.4	2
20	5.45	0.130	35.5	2
30	5.90	0.141	30.2	2
40	6.16	0.148	27.0	2
50	6.36	0.152	24.8	2
60	6.47	0.155	23.5	2
80	6.66	0.159	21.2	3
100	6.85	0.163	19.0	3
∞	---	0.170	15.0	---

TABLE 13

CAPILLARY PRESSURE CURVE DATA FOR CORE NO. 4 - 5

Berea Ss.

Bulk Volume = 40.55 cc
Pore Volume = 9.74 cc

P_c Cms. Hg.	Cumulative Displaced Vol. cc	S_{nw} as Fraction of Bulk Vol.	% S_w	Days to Equilibrium
5	0.0	0.0	100	3
8	1.94	0.048	80.0	2
10	3.86	0.095	60.4	2
15	5.72	0.141	41.3	2
20	6.56	0.162	32.5	2
30	7.10	0.175	27.2	2
40	7.31	0.180	25.0	2
50	7.39	0.182	24.2	2
60	7.51	0.185	22.9	2
80	7.67	0.189	21.2	3
100	7.91	0.195	18.7	3
∞	---	0.205	14.5	---

TABLE 14

CAPILLARY PRESSURE CURVE DATA FOR CORE NO. 4 - 8 USING MERCURY

Porosity = 24.5%

Bulk Volume of Plug = 28.76 - (21.52 - 10.94) = 18.18 cc

*Corrected Pressure P_c Psia	Hg. Fraction of Bulk Volume
3.9	(10.94 - 10.79) / 18.18 = 0.008
5.7	(10.94 - 10.75) / 18.18 = 0.010
8.5	(10.94 - 9.75) / 18.18 = 0.065
11.4	(10.94 - 8.65) / 18.18 = 0.126
13.6	(10.94 - 8.36) / 18.18 = 0.142
17.0	(10.94 - 8.01) / 18.18 = 0.161
22.0	(10.94 - 7.95) / 18.18 = 0.165
27.0	(10.94 - 7.89) / 18.18 = 0.168
55.0	(10.94 - 7.64) / 18.18 = 0.181
108.0	(10.94 - 7.45) / 18.18 = 0.192
316.0	(10.94 - 7.20) / 18.18 = 0.206

*Includes 1.5 psia to account for height of mercury above centre of core plug.

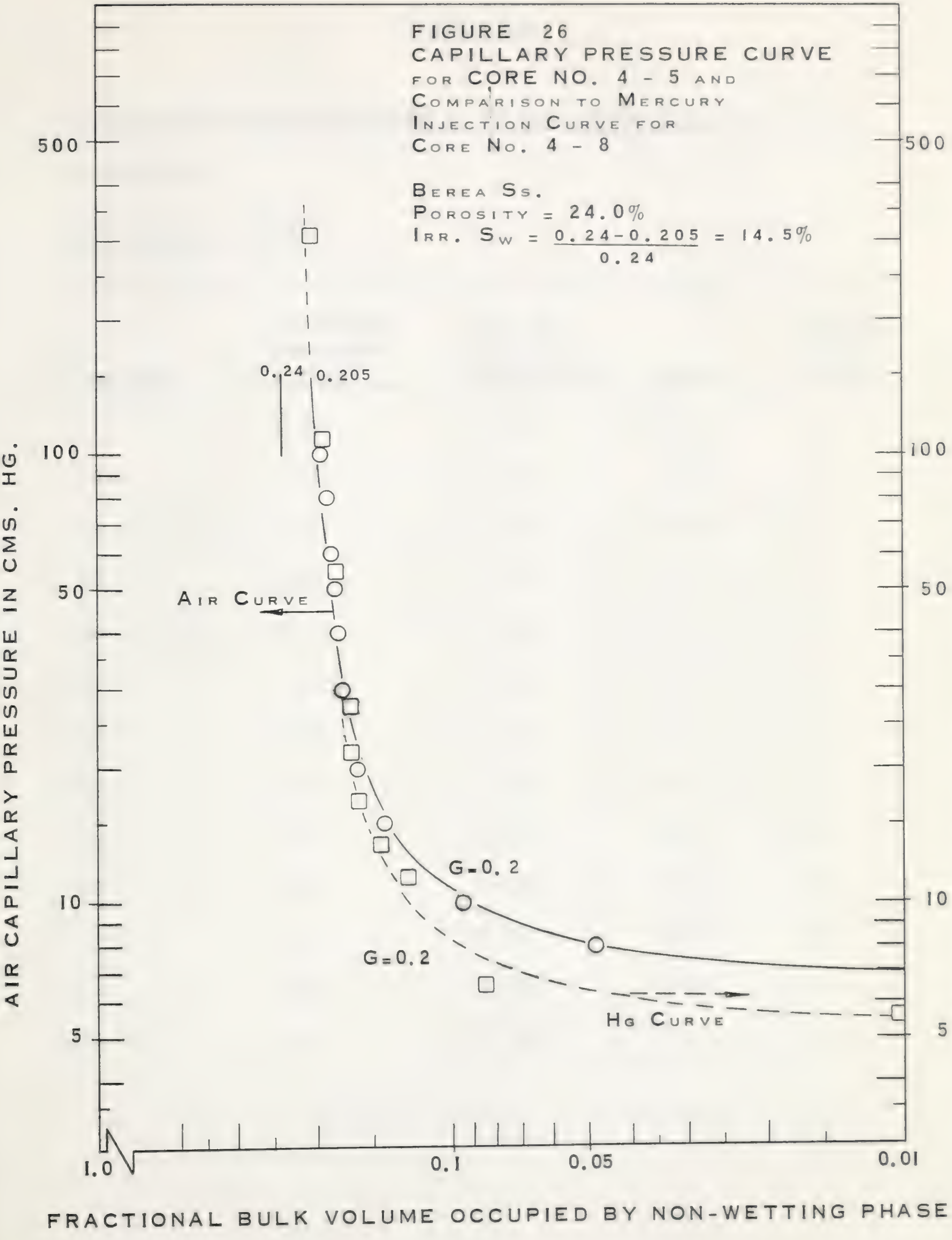

FIGURE 26
CAPILLARY PRESSURE CURVE
FOR CORE NO. 4 - 5 AND
COMPARISON TO MERCURY
INJECTION CURVE FOR
CORE NO. 4 - 8

BEREA SS.
POROSITY = 24.0%
IRR. $S_W = \frac{0.24-0.205}{0.24} = 14.5\%$

TABLE 15

CAPILLARY PRESSURE CURVE DATA FOR CORE NO. 5 - 2

Cardium Ss.

Bulk Volume = 40.55 cc
Pore Volume = 7.10 cc

P_c Cms. Hg.	Cumulative Displaced Vol. cc	S_{nw} as Fraction of Bulk Vol.	% S_w	Days to Equilibrium
5	0.00	0.00	100	3
10	0.57	0.014	91.9	3
15	3.52	0.087	50.3	3
20	4.42	0.109	37.7	3
30	5.18	0.128	27.1	2
40	5.23	0.129	26.3	2
50	5.27	0.130	25.7	2
60	5.31	0.131	25.1	2
70	5.39	0.133	24.1	2
80	5.47	0.135	22.8	2
90	5.51	0.136	22.3	2
100	5.64	0.139	20.6	3
∞	---	0.145	17.1	---

TABLE 16

CAPILLARY PRESSURE CURVE DATA FOR CORE NO. 5 - 4 USING MERCURY

Porosity = 19.0%

Bulk Volume of Plug = 28.76 - (21.61 - 10.43) = 17.58 cc

*Corrected Pressure P_c Psia	Hg. Fraction of Bulk Volume
9.8	(10.43 - 10.24) / 17.58 = 0.011
10.5	(10.43 - 10.15) / 17.58 = 0.016
11.7	(10.43 - 9.83) / 17.58 = 0.034
12.9	(10.43 - 9.59) / 17.58 = 0.048
15.4	(10.43 - 9.24) / 17.58 = 0.068
19.1	(10.43 - 8.99) / 17.58 = 0.082
28.0	(10.43 - 8.53) / 17.58 = 0.108
43.0	(10.43 - 8.25) / 17.58 = 0.124
66.0	(10.43 - 8.10) / 17.58 = 0.133
90.0	(10.43 - 8.01) / 17.58 = 0.138
174.0	(10.43 - 7.81) / 17.58 = 0.149
290.0	(10.43 - 7.75) / 17.58 = 0.153
460.0	(10.43 - 7.65) / 17.58 = 0.158

*Includes 1.5 psia to account for height of mercury above core plug.

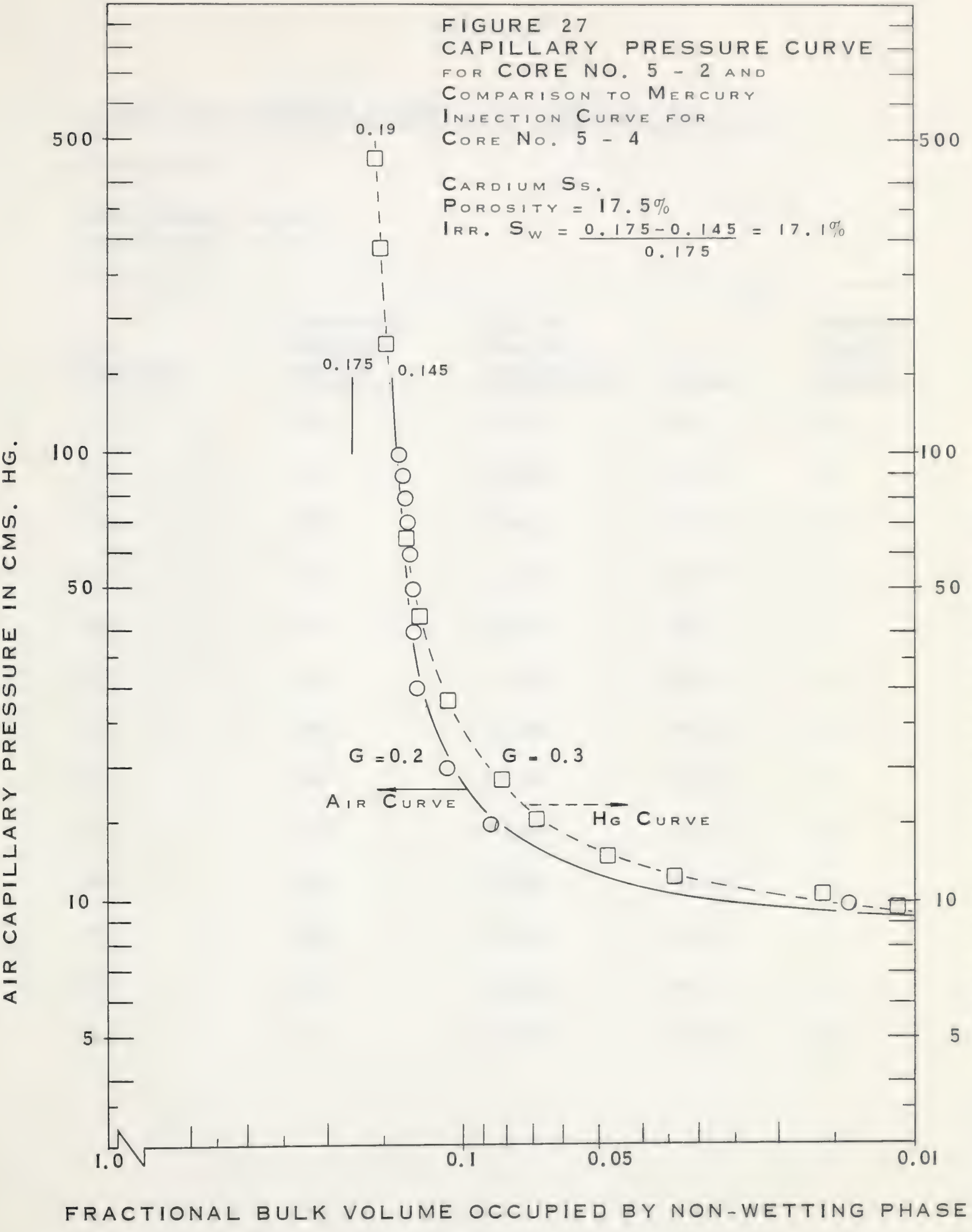

FIGURE 27
CAPILLARY PRESSURE CURVE
FOR CORE NO. 5 - 2 AND
COMPARISON TO MERCURY
INJECTION CURVE FOR
CORE NO. 5 - 4

CARDIUM SS.
POROSITY = 17.5%
IRR. $S_W = \frac{0.175-0.145}{0.175} = 17.1\%$

TABLE 17

CAPILLARY PRESSURE CURVE DATA FOR CORE NO. 7 - 3

Cardium Ss.

Bulk Volume = 40. 45
Pore Volume - 7. 19

P_c Cms. Hg.	Cumulative Displaced Vol. cc.	S_{nw} as Fraction of Bulk Vol.	% S_w	Days to Equilibrium
5	0. 00	0. 00	100	3
10	0. 73	0. 018	89. 8	3
15	3. 32	0. 082	53. 6	3
20	4. 16	0. 103	42. 2	3
30	4. 77	0. 118	33. 7	2
40	5. 06	0. 125	29. 6	2
50	5. 38	0. 132	25. 2	2
60	5. 46	0. 135	24. 0	2
70	5. 54	0. 137	23. 1	2
80	5. 62	0. 139	21. 8	2
90	5. 66	0. 140	21. 3	2
100	5. 70	0. 141	20. 7	3
∞	---	0. 145	18. 5	---

TABLE 18

CAPILLARY PRESSURE CURVE DATA FOR CORE NO. 7 - 4

Cardium Ss.

Bulk Volume = 40.65 cc
Pore Volume = 7.32 cc

P_c Cms. Hg.	Cumulative Displaced Vol. cc	S_{nw} as Fraction of Bulk Vol.	% S_w	Days to Equilibrium
5	0.00	0.00	100	3
10	0.45	0.011	93.9	3
15	3.38	0.083	53.8	3
20	4.39	0.108	40.0	3
30	5.20	0.128	27.6	2
45	5.53	0.136	24.4	2
50	5.65	0.139	22.8	2
60	5.73	0.141	21.7	2
70	5.81	0.143	20.6	2
80	5.85	0.144	20.2	2
90	5.89	0.145	19.6	2
100	5.93	0.146	19.0	3
∞	---	0.150	16.7	---

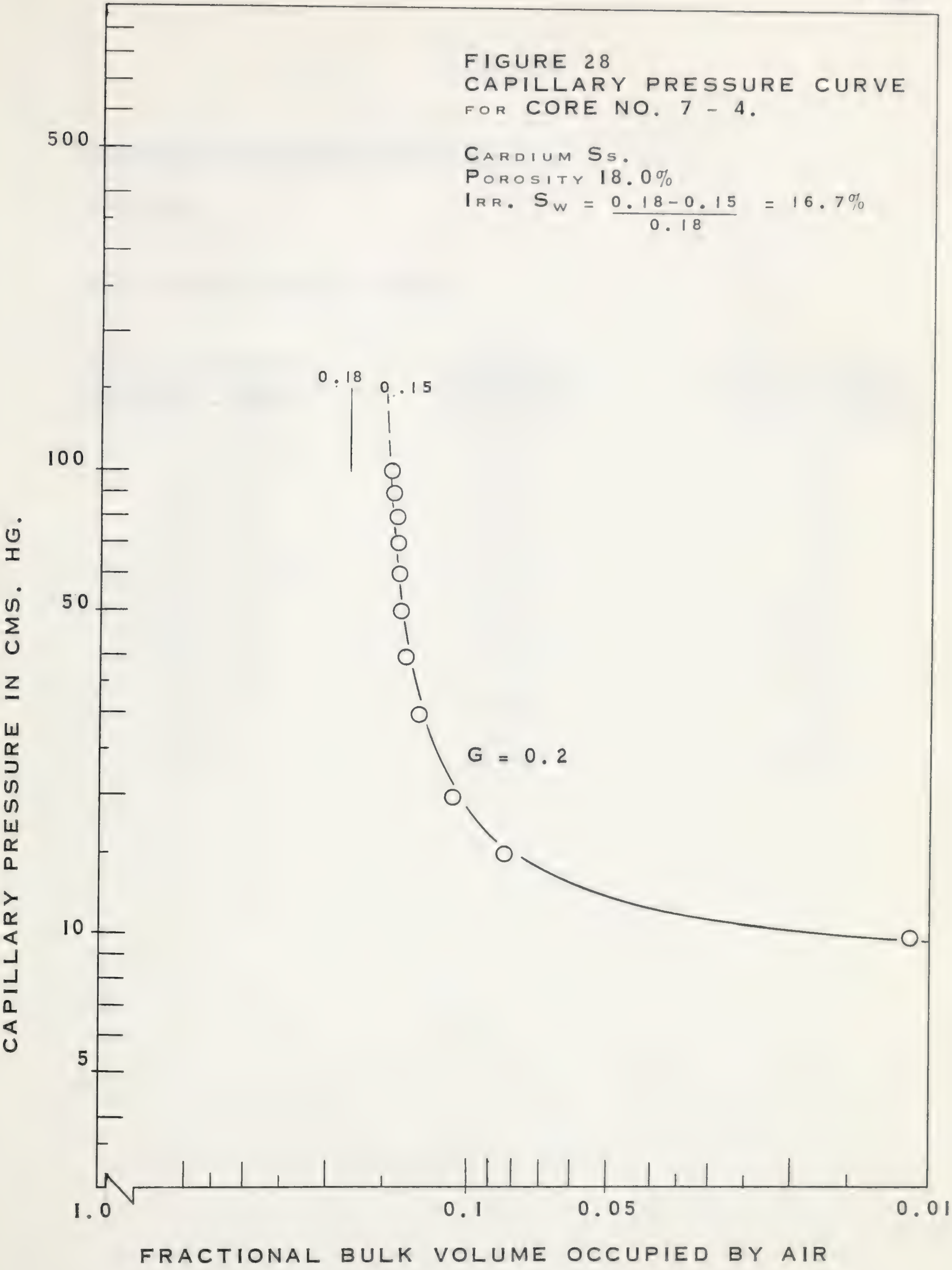

FIGURE 28
CAPILLARY PRESSURE CURVE
FOR CORE NO. 7 - 4.

Cardium Ss.
Porosity 18.0%
Irr. $S_W = \frac{0.18-0.15}{0.18} = 16.7\%$

TABLE 19

IMBIBITION DATA FOR CORE NO. 1 - 4

Berea Ss.

Pore Volume of Core = 7.73 cc

Time Since Start of Imbibition - mins.	Total Water Imbibed cc	Water Imbibed as % of Pore Vol.
5	1.5	19.5
10	2.6	33.7
17	2.9	37.5
27	3.2	41.3
37	3.3	42.8
52	3.35	43.4
82	3.45	44.7

TABLE 20

IMBIBITION DATA FOR CORE NO. 2 - 5

Indiana Ls.

Pore Volume of Core = 7.45 cc

Time Since Start of Imbibition - mins	Total Water Imbibed cc	Water Imbibed as % of Pore Vol.
5	0.75	10.1
11	1.60	21.5
16	2.10	28.2
23	2.70	36.2
31	3.00	40.2
42	3.20	43.0
58	3.30	44.3
71	3.40	45.7
86	3.45	46.4

TABLE 21

PERMEABILITY AND PLUGGING DATA FOR CORE NO. 1 - 1

Devonian Ls

Pore Volume = (4.9 x 8) 0.178 = 6.96 cc

STABILIZED PRESSURE PROFILE Pumping Brine:

PSIG				
Inlet	Tap 1	Tap 2	Tap 3	Outlet
310	288	255	220	200

$$K_i = \frac{0.139\,(0.725)\,8}{4.9\left(\frac{110}{14.7}\right)} \times 1000 = \underline{\underline{22.0}}\ \text{md}$$

PLUGGING DATA with Bacteria in Brine:

	PSIG						
Pore Vols. Injected	Inlet	Tap 1	Tap 2	Tap 3	Outlet	Total ΔP	K/K_i
14.4	328	293	257	220	200	128	0.86
43.1	418	319	259	220	200	218	0.51
64.7	468	331	263	221	200	268	0.41
101	632	363	268	220	200	432	0.26
136	711	380	269	219	200	511	0.22
187	833	389	274	220	200	633	0.18
209	952	407	275	221	200	752	0.15
230	1046	415	279	220	200	846	0.13
259	1112	446	282	221	200	912	0.12
288	1186	456	284	221	200	986	0.11

TABLE 22

PERMEABILITY AND PLUGGING DATA FOR CORE NO. 1 - 3

Devonian Ls.

Pore Volume = (4. 9 x 8) 0. 169 = 6. 62 cc

STABILIZED PRESSURE PROFILE Pumping Brine:

PSIG				
Inlet	Tap 1	Tap 2	Tap 3	Outlet
313	295	248	224	200

$$K_i = \frac{0.139\,(0.725)\,8}{4.9\left(\frac{113}{14.7}\right)} \times 1000 = \underline{\underline{21.4}}\ \text{md}$$

PLUGGING DATA with Bacteria in Brine:

	PSIG						
Pore Vols. Injected	Inlet	Tap 1	Tap 2	Tap 3	Outlet	Total ΔP	K/K_i
15. 1	346	313	249	224	200	146	0. 78
30. 2	378	326	251	224	200	178	0. 64
60. 4	420	380	258	224	200	220	0. 52
90. 6	542	496	266	223	200	342	0. 33
121	627	576	274	222	200	427	0. 27
148	690	668	280	222	200	490	0. 23
166	721	698	283	224	200	521	0. 22
182	756	732	287	224	200	556	0. 20
204	783	758	287	224	200	583	0. 19
227	812	785	289	224	200	612	0. 18

TABLE 23

PERMEABILITY AND PLUGGING DATA FOR CORE NO. 1 - 4

Devonian Ls.

Pore Volume = (4. 9 x 8) 0. 182 = 7. 14 cc

STABILIZED PRESSURE PROFILE Pumping Brine:

PSIG				
Inlet	Tap 1	Tap 2	Tap 3	Outlet
249	239	227	214	200

$$K_i = \frac{0.139\,(0.725)\,8}{4.9 \times \left(\frac{49}{14.7}\right)} \times 1000 = \underline{\underline{49.4}}\ \text{md}$$

PLUGGING DATA with Bacteria in Brine:

	PSIG						
Pore Vols. Injected	Inlet	Tap 1	Tap 2	Tap 3	Outlet	Total ΔP	K/K_i
14. 0	270	246	232	215	200	70	0. 70
28. 0	284	249	235	216	200	84	0. 59
49. 1	301	257	243	218	200	101	0. 49
63. 0	311	259	245	218	200	111	0. 44
105	344	261	247	218	200	144	0. 34
133	385	260	245	219	200	185	0. 27
161	395	256	242	220	200	195	0. 25
182	401	248	232	217	200	201	0. 24
203	407	250	233	218	200	207	0. 23
238	463	251	234	218	200	263	0. 19

TABLE 24

PERMEABILITY AND PLUGGING DATA FOR CORE NO. 2 - 2

Indiana Ls.

Pore Volume = (4. 9 x 8) 0. 195 = 7. 65 cc

STABILIZED PRESSURE PROFILE Pumping Brine:

PSIG				
Inlet	Tap 1	Tap 2	Tap 3	Outlet
480	391	329	229	50

$$K_i = \frac{0.139\,(0.725)\,8}{4.9\left(\frac{430}{14.7}\right)} \times 1000 = \underline{\underline{5.7}} \text{ md}$$

PLUGGING DATA with Bacteria in Brine:

	PSIG						
Pore Vols. Injected	Inlet	Tap 1	Tap 2	Tap 3	Outlet	Total Δ P	K/K_i
13. 1	528	412	338	228	50	478	0. 90
39. 2	560	406	332	228	50	510	0. 84
58. 8	642	438	342	224	50	592	0. 73
91. 6	682	444	364	242	50	632	0. 67
124	812	534	397	238	50	762	0. 58
157	877	517	389	241	50	827	0. 52
190	981	532	396	241	50	931	0. 46
210	1079	544	399	247	50	1029	0. 42
236	1212	568	412	248	50	1162	0. 37
274	1432	561	408	251	50	1382	0. 31
313	1628	577	419	252	50	1578	0. 27

TABLE 25

PERMEABILITY AND PLUGGING DATA FOR CORE NO. 2 - 4

Indiana Ls.

Pore Volume = (4.9 x 8) 0.190 = 7.45 cc

STABILIZED PRESSURE PROFILE Pumping Brine:

PSIG				
Inlet	Tap 1	Tap 2	Tap 3	Outlet
583	461	331	195	50

$$K_i = \frac{0.139\,(0.725)\,8}{4.9 \times \frac{(533)}{(14.7)}} \times 1000 = \underline{\underline{4.5 \text{ md}}}$$

PLUGGING DATA with Bacteria in Brine:

	PSIG						
Pore Vols. Injected	Inlet	Tap 1	Tap 2	Tap 3	Outlet	Total $\triangle P$	K/K_i
13.4	636	468	334	196	50	586	0.91
26.8	670	472	336	196	50	620	0.86
40.2	708	476	339	197	50	658	0.81
53.6	742	478	340	198	50	692	0.77
67.0	819	483	342	198	50	769	0.69
94.0	910	491	345	201	50	860	0.62
121	935	490	346	200	50	885	0.60
148	1036	499	351	202	50	986	0.54
175	1158	517	363	206	50	1108	0.48
215	1296	522	368	207	50	1246	0.43
255	1452	538	372	207	50	1402	0.38
282	1646	564	377	209	50	1596	0.33

TABLE 26

PERMEABILITY AND PLUGGING DATA FOR CORE NO. 2 - 5

Indiana Ls.

Pore Volume = (4.9 x 8) 0.185 = 7.25 cc

STABILIZED PRESSURE PROFILE Pumping Brine:

PSIG				
Inlet	Tap 1	Tap 2	Tap 3	Outlet
552	426	300	174	50

$$K_i = \frac{0.139\,(0.725)\,8}{4.9\left(\frac{502}{14.7}\right)} \times 1000 = \underline{\underline{4.8}}\text{ md}$$

PLUGGING DATA with Bacteria in Brine:

Pore Vols. Injected	PSIG						
	Inlet	Tap 1	Tap 2	Tap 3	Outlet	Total $\triangle$P	K/Ki
13.8	610	427	301	175	50	560	0.90
27.6	648	429	301	176	50	598	0.84
41.4	685	430	303	177	50	635	0.79
55.2	765	432	303	178	50	715	0.70
68.9	836	435	304	178	50	786	0.64
96.6	992	441	307	181	50	942	0.54
124	1148	442	307	181	50	1098	0.46
138	1260	444	309	182	50	1210	0.41
166	1416	447	310	182	50	1366	0.37
194	1588	450	312	182	50	1538	0.33
221	1720	454	314	183	50	1670	0.30
248	1915	459	318	184	50	1865	0.26

TABLE 27

PERMEABILITY AND PLUGGING DATA FOR CORE NO. 2 - 6

Indiana Ls.

Pore Volume = (4.9 x 8) 0.20 = 7.84 cc

STABILIZED PRESSURE PROFILE Pumping Brine:

PSIG				
Inlet	Tap 1	Tap 2	Tap 3	Outlet
559	421	307	188	50

$$K_i = \frac{0.139\,(0.725)\,8}{4.9 \times \left(\frac{509}{14.7}\right)} \times 1000 = \underline{\underline{4.8}}\ \text{md}$$

PLUGGING DATA with Bacteria in Brine:

	PSIG						
Pore Vols. Injected	Inlet	Tap 1	Tap 2	Tap 3	Outlet	Total ΔP	K/K_i
12.7	596	422	306	188	50	546	0.93
25.5	691	424	308	189	50	641	0.79
38.3	656	424	308	188	50	606	0.84
57.4	847	427	310	190	50	797	0.64
89.4	885	430	310	190	50	835	0.61
121	1070	445	315	190	50	1020	0.50
153	1246	451	318	192	50	1196	0.43
178	1307	453	317	191	50	1257	0.41
217	1330	455	319	192	50	1280	0.40
255	1445	457	321	193	50	1395	0.36
293	1592	460	323	195	50	1542	0.33
319	1743	464	324	196	50	1693	0.29

TABLE 28

PERMEABILITY AND PLUGGING DATA FOR CORE NO. 4 - 1

Berea Ss.

Pore Volume = (4.9 x 8) 0.19 = 7.45 cc

STABILIZED PRESSURE PROFILE Pumping Brine:

PSIG				
Inlet	Tap 1	Tap 2	Tap 3	Outlet
536	527	518	509	500

$$K_i = \frac{0.139\ (0.725)\ 8}{4.9 \times \left(\frac{36}{14.7}\right)} \times 1000 = \underline{\underline{67.2}}\ \text{md}$$

PLUGGING DATA with Bacteria in Brine:

	PSIG						
Pore Vols. Injected	Inlet	Tap 1	Tap 2	Tap 3	Outlet	Total ΔP	K/K_i
13.4	540	527	518	509	500	40	0.90
26.8	545	529	518	509	500	45	0.80
53.7	555	530	518	509	500	55	0.65
80.6	563	530	518	509	500	63	0.54
108	576	531	518	509	500	76	0.46
134	595	531	518	509	500	95	0.38
161	612	532	518	509	500	112	0.32
188	638	533	518	509	500	138	0.26
215	671	533	518	509	500	171	0.21
242	700	535	518	509	500	200	0.18
269	740	536	518	509	500	240	0.15

TABLE 29

PERMEABILITY AND PLUGGING DATA FOR CORE NO. 4 - 3

Berea Ss.

Pore Volume = (4. 9 x 8) 0. 225 = 8. 80 cc

STABILIZED PRESSURE PROFILE Pumping Brine:

P S I G				
Inlet	Tap 1	Tap 2	Tap 3	Outlet
516	511	507	503	500

$$K_i = \frac{0.139\,(0.725)\,8}{4.9 \times \left(\frac{16}{14.7}\right)} \times 1000 = \underline{\underline{151}}\ \text{md}$$

PLUGGING DATA with Bacteria in Brine:

	P S I G						
Pore Vols. Injected	Inlet	Tap 1	Tap 2	Tap 3	Outlet	Total Δ P	K/K_i
11. 4	518	511	507	503	500	18	0. 89
34. 1	519	511	507	503	500	19	0. 84
51. 1	521	512	507	503	500	21	0. 76
85. 2	525	513	507	503	500	25	0. 64
108	530	515	508	503	500	30	0. 53
171	545	515	508	503	500	45	0. 36
205	551	516	509	503	500	51	0. 31
238	558	516	509	503	500	58	0. 28
273	566	518	510	503	500	66	0. 24
307	571	519	510	503	500	71	0. 225
341	584	520	511	503	500	84	0. 191

TABLE 30

PERMEABILITY AND PLUGGING DATA FOR CORE NO. 4 - 5

Berea Ss.

Pore Volume = (4.9 x 8) 0.24 = 9.38 cc

STABILIZED PRESSURE PROFILE Pumping Brine:

P S I G				
Inlet	Tap 1	Tap 2	Tap 3	Outlet
510	507	505	502	500

$$K_i = \frac{0.139\,(0.725)\,8}{4.9 \times \left(\frac{10}{14.7}\right)} \times 1000 = \underline{\underline{242}}\ \text{md}$$

PLUGGING DATA with Bacteria in Brine:

	P S I G						
Pore Vols. Injected	Inlet	Tap 1	Tap 2	Tap 3	Outlet	Total ΔP	K/K_i
10.7	511	507	505	502	500	11	0.91
32.0	513	507	505	502	500	13	0.77
53.3	518	508	505	502	500	18	0.56
80.0	524	509	506	502	500	24	0.42
106	529	511	507	502	500	29	0.35
133	535	511	507	502	500	35	0.29
160	541	513	508	502	500	41	0.25
187	545	514	508	502	500	45	0.22
213	551	515	508	502	500	51	0.196
240	558	515	508	502	500	58	0.172
267	564	517	509	503	500	64	0.156
321	572	518	509	503	500	72	0.139

TABLE 31

PERMEABILITY AND PLUGGING DATA FOR CORE NO. 4 - 6

Berea Ss.

Pore Volume - (4. 9 x 8) 0. 22 - 8. 63 cc

STABILIZED PRESSURE PROFILE Pumping Brine:

PSIG				
Inlet	Tap 1	Tap 2	Tap 3	Outlet
525	518	512	506	500

$$K_i = \frac{0.139\,(0.725)\,8}{4.9 \times \left(\frac{25}{14.7}\right)} \times 1000 - \underline{\underline{96.8}} \text{ md}$$

PLUGGING DATA with Bacteria in Brine:

	PSIG						
Pore Vols. Injected	Inlet	Tap 1	Tap 2	Tap 3	Outlet	Total $\triangle P$	K/K_i
11. 5	528	518	512	506	500	28	0. 89
34. 8	538	519	513	506	500	38	0. 66
52. 2	546	521	514	507	500	46	0. 54
69. 5	554	521	514	507	500	54	0. 46
87. 0	561	524	514	507	500	61	0. 41
104	569	525	514	507	500	69	0. 37
145	584	525	514	507	500	84	0. 30
197	600	528	515	507	500	100	0. 25
267	621	531	516	508	500	121	0. 206
318	646	533	518	508	500	146	0. 171
348	659	535	519	508	500	159	0. 157

TABLE 32

PERMEABILITY AND PLUGGING DATA FOR CORE NO. 5 - 2

Cardium Ss.

Pore Volume = (4.9 x 8) 0.175 = 6.85 cc

STABILIZED PRESSURE PROFILE Pumping Brine:

P S I G				
Inlet	Tap 1	Tap 2	Tap 3	Outlet
358	343	329	314	300

$$K_i = \frac{0.139\,(0.725)\,8 \times 1000}{4.9 \times \left(\frac{58}{14.7}\right)} = \underline{\underline{41.8}} \text{ md}$$

PLUGGING DATA with Bacteria in Brine:

	P S I G						
Pore Vols. Injected	Inlet	Tap 1	Tap 2	Tap 3	Outlet	Total Δ P	K/K_i
14.6	364	341	330	314	300	64	0.91
29.2	370	342	331	312	300	70	0.83
43.8	376	342	331	313	300	76	0.76
72.9	394	343	329	315	300	94	0.62
102	431	343	328	315	300	131	0.44
131	470	342	328	313	300	170	0.34
160	507	342	329	314	300	207	0.28
182	563	343	330	314	300	263	0.22
204	590	342	329	312	300	290	0.20
219	607	342	329	312	300	307	0.19

TABLE 33

PERMEABILITY AND PLUGGING DATA FOR CORE NO. 5-3

Cardium Ss.

Pore Volume = (4.9 x 8) 0.187 = 7.32 cc

STABILIZED PRESSURE PROFILE Pumping Brine:

P S I G				
Inlet	Tap 1	Tap 2	Tap 3	Outlet
355	340	327	313	300

$$K_i = \frac{0.139\,(0.725)\,8}{4.9 \times \left(\frac{55}{14.7}\right)} \times 1000 = \underline{44.1} \text{ md}$$

PLUGGING DATA with Bacteria in Brine:

	P S I G						
Pore Vols. Injected	Inlet	Tap 1	Tap 2	Tap 3	Outlet	Total ΔP	K/K_i
13.6	360	342	328	314	300	60	0.91
27.3	367	342	327	313	300	67	0.82
40.9	376	343	328	313	300	76	0.72
68.4	398	344	329	312	300	98	0.56
95.5	438	345	329	313	300	138	0.40
123	477	345	330	312	300	177	0.31
150	528	345	330	312	300	228	0.24
177	560	346	331	312	300	260	0.21
204	589	347	331	312	300	289	0.19
232	624	347	331	312	300	324	0.17

TABLE 34

PERMEABILITY AND PLUGGING DATA FOR CORE NO. 7 - 3

Cardium Ss.

Pore Volume = (4.9 x 8) 0.178 = 6.97 cc

STABILIZED PRESSURE PROFILE Pumping Brine:

PSIG				
Inlet	Tap 1	Tap 2	Tap 3	Outlet
339	328	319	310	300

$$K_i = \frac{0.139\,(0.725)\,8}{4.9 \times \left(\frac{39}{14.7}\right)} \times 1000 = \underline{\underline{57.7}} \text{ md}$$

PLUGGING DATA with Bacteria in Brine:

Pore Vols. Injected	PSIG					Total ΔP	K/K_i
	Inlet	Tap 1	Tap 2	Tap 3	Outlet		
14.3	346	329	320	311	300	46	0.85
28.6	357	329	320	311	300	57	0.69
46.6	380	330	320	311	300	80	0.49
64.6	400	331	321	312	300	100	0.39
82.5	413	330	321	312	300	113	0.35
101	427	329	320	311	300	127	0.31
118	451	330	320	311	300	151	0.26
136	472	330	321	312	300	172	0.23
165	503	330	321	312	300	203	0.19
194	548	331	320	312	300	248	0.16
215	574	331	321	312	300	274	0.14

TABLE 35

PERMEABILITY AND PLUGGING DATA FOR CORE NO. 7 - 4

Cardium Ss.

Pore Volume = (4.9 x 8) 0.18 = 7.05 cc

STABILIZED PRESSURE PROFILE Pumping Brine:

PSIG				
Inlet	Tap 1	Tap 2	Tap 3	Outlet
350	336	324	313	300

$$K_i = \frac{0.139\,(0.725)\,8}{4.9\left(\frac{50}{14.7}\right)} \times 1000 = \underline{\underline{48.5}} \text{ md}$$

PLUGGING DATA with Bacteria in Brine:

	PSIG						
Pore Vols. Injected	Inlet	Tap 1	Tap 2	Tap 3	Outlet	Total ΔP	K/K_i
14.2	358	338	325	313	300	58	0.86
28.4	366	338	325	313	300	66	0.76
42.6	375	337	324	313	300	75	0.67
71.0	391	335	322	312	300	91	0.55
99.5	416	337	324	313	300	116	0.43
120	431	335	322	312	300	131	0.38
142	447	336	323	312	300	147	0.34
170	492	337	324	313	300	192	0.26
192	507	335	323	312	300	207	0.24
213	526	334	322	312	300	226	0.22

TABLE 36

BACKWASHING DATA ON CORE NO. 1 - 3

Devonian Ls.

Injection Rate 1200 cc/hr with Brine

	PSIG						
Pore Vols. Injected	Inlet	Tap 1	Tap 2	Tap 3	Outlet	Total ΔP	K/K_i
15.1	760	702	540	197	50	710	0.38
30.2	695	637	522	181	50	645	0.42
60.4	624	566	480	174	50	574	0.47
90.6	560	501	417	159	50	510	0.53
151	482	424	334	141	50	432	0.63
227	426	368	289	120	50	376	0.72
378	394	335	264	118	50	344	0.79
453	373	313	248	115	50	323	0.84
538	357	297	232	110	50	307	0.88
604	350	289	232	109	50	300	0.90

TABLE 37

BACKWASHING DATA ON CORE NO. 2 - 6

Indiana Ls.

Injection Rate 500 cc/hr with Brine

	PSIG						
Pore Vols. Injected	Inlet	Tap 1	Tap 2	Tap 3	Outlet	Total Δ P	K/K_i
12.7	1230	1090	964	834	50	1180	0.43
25.4	1108	968	842	714	50	1058	0.48
51.1	960	820	694	575	50	910	0.56
76.6	844	704	580	461	50	794	0.64
102	728	589	465	345	50	678	0.75
127	661	521	399	279	50	611	0.83
153	642	503	382	265	50	592	0.86
205	615	475	355	240	50	565	0.90
255	608	469	350	235	50	558	0.91
319	602	463	345	230	50	552	0.92

TABLE 38

BACKWASHING DATA ON CORE NO. 4 - 3

Berea Ss.

Injection Rate = 1200 cc/hr with Brine

Pore Vols. Injected	PSIG Inlet	Tap 1	Tap 2	Tap 3	Outlet	Total $\triangle P$	K/K_i
11.4	111	102	94	86	50	61	0.64
22.7	109	100	92	84	50	59	0.65
45.4	107	98	90	82	50	57	0.67
90.8	104	96	88	80	50	54	0.72
125	101	93	85	77	50	51	0.76
171	99	91	83	75	50	49	0.79
205	97	89	81	73	50	47	0.82
242	95	87	79	71	50	45	0.84
284	94	86	78	70	50	44	0.85
342	93	85	77	69	50	43	0.87
398	92	84	76	68	50	42	0.88

TABLE 39

BACHWASHING DATA ON CORE NO. 5 - 3

Cardium Ss.

Injection Rate = 1200 cc/hr with Brine

	PSIG						
Pore Vols. Injected	Inlet	Tap 1	Tap 2	Tap 3	Outlet	Total ΔP	K/K_i
13.6	337	305	271	232	50	287	0.46
27.6	314	283	249	210	50	264	0.50
68.4	278	247	213	174	50	228	0.58
109	249	219	185	146	50	199	0.66
149	228	197	164	126	50	178	0.74
190	219	188	155	117	50	169	0.78
231	207	175	142	104	50	157	0.84
272	203	172	139	102	50	153	0.86
340	200	169	136	99	50	150	0.88
407	196	165	132	95	50	146	0.90

B29802